Minerals Engineering 247 (2026) 110496

Contents lists available at ScienceDirect

Minerals Engineering

journal homepage: www.elsevier.com/locate/mineng

Activating the hidden potential of mine tailings: A mineral-based mechanical activation framework

Berika Ceren Cihan Yılmaz [a,*], Demetrios M. Cotsovos [a], Gavin Mudd [b], Richard J. Ball [c], Ceren Ince [a]

[a] Institute for Sustainable Built Environment,School of Energy, Geoscience, Infrastructure and Society,Heriot-Watt University, Edinburgh, United Kingdom
[b] British Geological Survey, Critical Minerals Intelligence Centre,Nottingham, United Kingdom
[c] Centre for Integrated Materials, Processes & Structures (IMPS), Department of Architecture and Civil Engineering, Faculty of Engineering and Design,University of Bath, Bath, United Kingdom

ARTICLE INFO

Keywords:
Mine tailings valorisation
Mechanical activation
Mineralogical fingerprint
Decision-oriented framework
Energy efficiency
Cementitious materials
Circular economy

ABSTRACT

Mine tailings, produced at rates exceeding 10 billion tonnes annually, constitute the world's largest industrial waste stream. Catastrophic failures have caused loss of life, contamination, and long-term ecological harm, underscoring the need for sustainable and systematic management strategies. Yet they also represent an untapped resource for sustainable construction. Unlocking this potential requires activation techniques capable of generating reactive phases, as well as decision frameworks that can guide their responsible deployment. Therefore, this study introduces a mineral-based mechanical activation framework that supports informed evaluation of the activation behaviour and valorisation potential of mine tailings. The framework classifies minerals by their potential cementitious contribution following mechanical activation and their susceptibility to amorphisation, based on intrinsic mineralogical attributes. Case studies on multi-mineral mine tailings demonstrate broad consistency with the proposed framework: silica–alumina contributor group–dominated tailings tend to enhance pozzolanic reactivity, oxide contributor group–dominated tailings generally show limited response, and unsuitable mineral group–dominated tailings largely remain inert under mechanical activation. The framework provides a basis for mechanical activation as a systematic, design-informed decision strategy rather than an ad hoc empirical practice, grounded in the mineralogical fingerprint of mine tailings. Its mineralogical basis also offers a transferable conceptual basis for evaluating other industrial residues, providing a generic template for resource-efficient valorisation. The framework supports a shift in tailings utilisation away from a linear take–make–dispose paradigm toward more knowledge-driven evaluation and utilisation strategies, enabling more systematic assessment across waste streams and alignment with circular-economy and net-zero targets. Illustratively, enabling a ~ 15% substitution across 1 million tonnes of cement would valorise ~ 0.15 Mt of residues and avoid ~ 0.09–0.12 Mt CO_2.

1. Introduction

The global transition toward net-zero is accelerating the demand for critical minerals, driven by the rapid deployment of electrification and digital infrastructure. (OECD., 2018; Vidal et al., 2013). Metals such as copper, lithium, cobalt, and nickel have become indispensable to low-carbon technologies ranging from electric vehicle batteries and renewable energy systems to smart grids and data centers (Jasansky et al., 2023; Nguyen et al., 2021; Anglo American, n.d.). Between 2000 and 2023, global mineral production increased by more than 70%, and projections suggest that meeting the material demands of the energy transition could require up to 6 billion tonnes of metal by 2050 (Reichl and Schatz, 2025; ,World Gold Council, n.d.; OECD., 2024; Copper demand set to soar 70% by, 2050). This unprecedented expansion of mineral extraction, however, comes at a steep environmental cost: mining generates vast quantities of solid waste, with current estimates indicating ~ 90 billion tonnes of waste rock and 8 billion tonnes of tailings annually, contributing to a cumulative global volume exceeding

* Corresponding author at: Institute for Sustainable Built Environment, School of Energy, Geoscience, Infrastructure and Society, Heriot-Watt UniversityEdinburgh, United Kingdom.
E-mail address: bcc3000@hw.ac.uk (B.C. Cihan Yılmaz).

https://doi.org/10.1016/j.mineng.2026.110496
Received 7 February 2026; Received in revised form 27 May 2026; Accepted 3 June 2026
Available online 10 June 2026

640 billion m^3 (Humphreys, 2020; Global Tailings Portal, n.d.). Tailings that are rich in sulphides and heavy metals pose long-term risks to ecosystems and public health, primarily through acid mine drainage, groundwater contamination, and particulate emissions. (Concas et al., 2006; Budianta, 2021; Li et al., 2024; Lottermoser, 2011; Serbula et al., 2017; Afif et al., 2008). Despite reliance on tailings storage facilities (TSFs), catastrophic failures such as the Brumadinho disaster underscore the urgent need for alternative, sustainable management strategies (Piciullo et al., 2022; Islam and Murakami, 2021; Chronology of major tailings dam failures, n.d.).

A parallel sustainability challenge lies in cement production, which contributes ~ 8% of global anthropogenic CO_2 emissions, primarily from limestone calcination and clinker production (CBS News, n.d.). In this dual context, valorising mine tailings in cementitious matrices has gained prominence as a synergistic solution; simultaneously mitigating mining's environmental burden and reducing the carbon footprint of construction materials (CBS News, n.d.; Kinnunen et al., 2022; Scrivener et al., 2018). Such valorisation strategies of this kind hold direct relevance for industry stakeholders and policymakers, providing actionable pathways to integrate utilisation of tailings into broader decarbonisation efforts. Yet, despite growing interest, implementation remains fragmented. Mine tailings exhibit extreme variability in mineralogy, particle size, and chemical composition due to differences in ore type, extraction, processing route, and environmental exposure (Lottermoser, 2010; González-Díaz et al., 2022; Falagán et al., 2017; Fashola et al., 2016; Hu et al., 2017; Nascimento et al., 2023). Tailings nominally derived from similar metal extraction processes can behave inconsistently in binder systems (Lottermoser, 2010), as variations in ore mineralogy and processing routes lead to diverse results across studies (Saberi and Vriens, 2025; Lindsay et al., 2015; Nascimento et al., 2025) and hinder scalability. The root cause of these inconsistencies lies in the absence of a standardized, mineralogically informed framework for evaluating tailings in binder applications. To address this gap, a classification taxonomy is defined based on structural state, chemical composition, fineness, and toxicity, aligned with international standards (e.g., Code of Federal Regulations (CFR) (40 CFR § 261.24, n.d.), Waste Classification Technical Guidance WM3 (Agency et al., 2021), ASTM C618 (ASTM International., 2023), ASTM C1866 (ASTM International., 2020), and BS EN 450–1 (British Standards Institution, 2012). This taxonomy provided a first-stage screening method, distinguishing tailings with intrinsic reactivity, latent pozzolanic potential, inert character, or unsuitability without pretreatment. However, for tailings with activation potential, chemical and physical metrics alone are insufficient; bridging the taxonomy with mineralogical insight becomes necessary to capture the mechanisms that govern reactivity. In particular, the type, proportion, and structural characteristics of constituent minerals ultimately control both the reactivity of tailings and the effectiveness of activation strategies. Despite this importance, the relationship between mineralogical composition and activation effectiveness remains insufficiently understood, and a mineral-based perspective systematically linking mineral properties with activation behaviour is largely absent in studies addressing heterogeneous materials such as mine tailings.

Among the activation techniques proposed to enhance the reactivity of mine tailings, mechanical activation has emerged as a promising low-carbon approach. However, the effectiveness of this process is highly mineral-dependent. In the absence of a clear mechanistic understanding of how mineralogical composition governs activation behaviour, mechanical activation has often been applied empirically, leading to inconsistent outcomes across studies. For example, quartz- or hematite-rich tailings typically exhibit only limited reactivity (Wang et al., 2023; Liu et al., 2022), while those dominated by muscovite or kaolinite can develop significant pozzolanic activity after milling (Wang et al., 2022; Yao et al., 2019; Yao et al., 2020; Tian et al., 2024). This variability highlights a fundamental knowledge gap: unlocking the reactivity of mine tailings requires understanding how the mineralogical characteristics of their constituent phases influence their response to activation.

Mine tailings are inherently complex multimineral assemblages composed of multiple coexisting mineral phases. In such heterogeneous systems, interactions among mineral phases may have an influence on the activation behaviour and can give rise to synergistic or antagonistic effects depending on mineralogical composition and relative phase abundance. These interactions may affect processes such as the efficiency of mechanical energy transfer during milling, fracture behaviour and structural breakdown, the extent of amorphisation, dissolution tendencies, and the resulting surface reactivity of the activated material (Baláž, 2008). Consequently, interpreting the activation behaviour of heterogeneous mine tailings requires understanding the structural characteristics and activation responses of the individual mineral phases that constitute these systems.

In this context, the primary aim of the present study is to develop a mineralogical framework capable of explaining the mechanisms governing mechanical activation in mine tailings from a mineral-level perspective. To achieve this, the study proposes a mineral-based mechanical activation framework that systematically links mineral properties with activation behaviour. By integrating crystallographic structure, bonding topology, interlayer bonding characteristics, hardness, cleavage, and mineral-specific behaviour under milling, the framework systematically classifies minerals according to both their functional contribution to cementitious matrices and their susceptibility to structural breakdown during mechanical activation. Therefore, the study introduces a mineralogical perspective that is currently lacking in the literature on mine tailings in cementitious systems and provides a foundation for interpreting activation behaviour in a more mechanistic and consistent manner. Establishing this mineral-level understanding represents a necessary step toward transforming mechanical activation from an empirical trial-and-error practice into a mechanistically guided strategy for the valorisation of heterogeneous mine tailings.

Ultimately, this framework reconceptualises mechanical activation not as a generic treatment but as a tailored, mineral-specific engineering tool for valorising heterogeneous mine tailings. Consequently, it supports circular-economy objectives and can contribute toward net-zero strategies by enabling a more systematic approach to the valorisation of mine tailings in sustainable binder systems. In practical terms, the framework provides a structured basis that can support regulators, standards bodies, and industry practitioners in systematically evaluating valorisation pathways.

2. Database development and methodology

This study is based on a comprehensive literature-derived database designed to represent the existing body of research on the utilisation of mine tailings in cementitious systems. Relevant publications were sourced from major scientific databases, including Scopus, ScienceDirect, Springer, and Taylor & Francis, using a unified keyword strategy. The search scope was deliberately defined to ensure broad and representative coverage of the relevant literature.

As illustrated in the PRISMA-style flow diagram (Fig. 1), the literature identification and screening process followed a multi-stage refinement procedure. The initial search identified more than 5000 publications addressing mine tailings in cementitious systems. Following title and abstract screening, studies that did not meet the defined scope of the research were excluded, leaving 849 articles for full-text eligibility assessment. After applying predefined inclusion and exclusion criteria, a curated database of 175 peer-reviewed journal articles was established. This curated database encompasses a wide range of studies examining different utilisation pathways for mine tailings, including direct use and various treatment approaches such as mechanical, thermal, and chemical activation.

For the purposes of the present study, which focuses specifically on mechanical activation, this database was further refined through two additional selection criteria: studies were required to report the mineralogical composition of the tailings (e.g., via X-ray diffraction (XRD) or

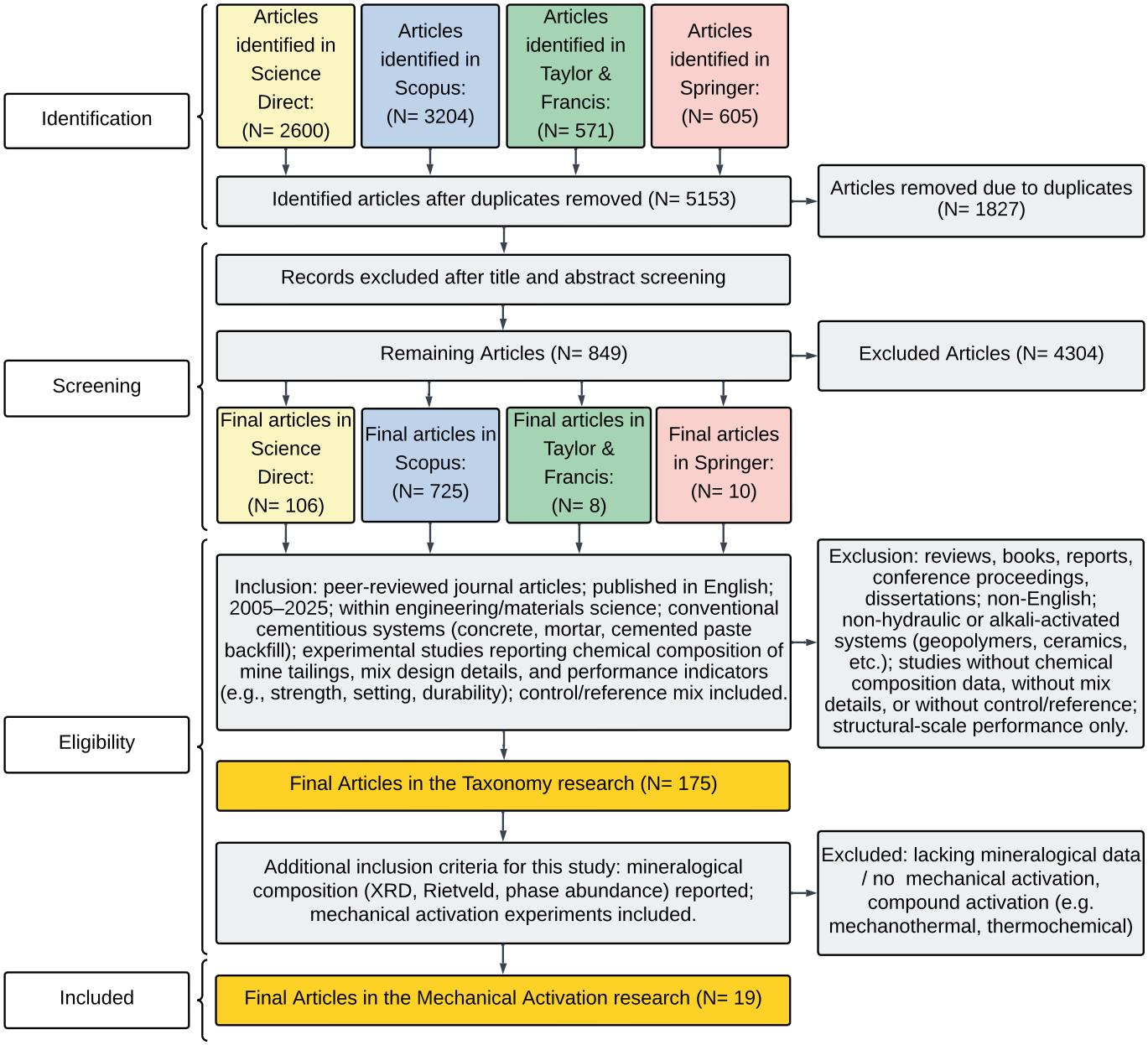

Fig. 1. PRISMA-style flow diagram of study selection and refinement process.

Rietveld analysis) and to include experimental evaluation of mechanical activation prior to cementitious application. Applying these criteria resulted in a final dataset of 19 studies.

This outcome reflects a broader limitation within existing literature. While mechanical activation of mine tailings has been widely explored, the majority of studies do not provide mineralogical characterization at a resolution sufficient to enable phase-specific interpretation of activation behaviour. Consequently, the relationship between mineralogical assemblage, mechanochemical response, and resulting cementitious reactivity remains insufficiently constrained, and current approaches to mechanical activation design remain largely empirical, with limited mineralogical and mechanistic grounding. In addition, milling conditions and activation parameters are often reported inconsistently, limiting meaningful cross-comparison between datasets. The resulting dataset of only 19 studies therefore highlights the broader scarcity of mineralogically interpretable mechanical activation datasets within the current literature.

Nevertheless, the selected studies collectively encompass a broad range of mineral phases commonly encountered in mine tailings, enabling evaluation of the proposed framework across diverse mineralogical contexts.

The selected studies were used to assess the capability of the proposed mineral-based framework. The framework was developed based on representative mineral phases commonly occurring in mine tailings systems identified within the broader literature dataset. This enabled evaluation of how different mineralogical assemblages influence activation outcomes in cementitious systems by comparing expected mineral-level responses with reported experimental performance.

3. From classification to activation: Unlocking the reactivity of mine tailings through mineralogical insights and activation strategies

Mine tailings, owing to their chemically rich composition, exhibit strong similarities with cement and supplementary cementitious materials (SCMs), making them promising candidates for use in binder

systems. However, their chemical, physical, and mineralogical characteristics vary widely with ore type, extraction and processing methods, geographical origin, and environmental exposure (Lottermoser, 2010; González-Díaz et al., 2022; Falagán et al., 2017; Fashola et al., 2016; Hu et al., 2017; Nascimento et al., 2023). This heterogeneity yields tailings that may be amorphous, partly amorphous, or predominantly crystalline, often resulting in inconsistent performance when used directly or even after activation. While chemical composition provides an initial indication of whether a tailing can act as a reactive precursor or merely as an inert filler, its actual response to activation is governed primarily by mineralogical assemblage. Hence, unlocking the latent reactivity of mine tailings requires a mechanistic understanding of how different mineral phases respond to activation.

To address this, the present study introduces a mineralogical evaluation stage within the activation decision-making process, establishing a framework that connects initial classification with mineral-specific activation strategies (Fig. 2). The resulting framework follows five structured stages that integrate chemical, physical, and mineralogical data into a coherent evaluation pathway. In the first stage, raw tailings are screened against established environmental thresholds and compositional benchmarks derived from existing standards commonly used in the evaluation of supplementary cementitious materials (SCMs), since mine tailings intended for cementitious applications are ultimately evaluated according to their ability to function as reactive or supplementary binder constituents within cementitious systems. Environmental and toxicity-related limitations were evaluated based on CFR (40 CFR § 261.24, n.d.) and WM3 (Agency et al., 2021), oxide-based compositional classifications were referenced from ASTM C618 (ASTM International., 2023), amorphous phase criteria were informed by ASTM C1866 (ASTM International., 2020), and silica-related compositional benchmarks were adopted from BS EN 450–1 (British Standards Institution, 2012). Physical parameters related to particle size and processability were also incorporated into the screening stage.

This initial screening stage assigns tailings to taxonomy groups that distinguish between materials suitable for direct use, those requiring activation, and those unsuitable due to chemical deficiencies or environmental constraints. Accordingly, the taxonomy stage functions as a preliminary classification and valorisation-screening approach prior to detailed mineralogical evaluation and activation-oriented assessment.

It should be emphasised that the compositional and physical thresholds incorporated into the preliminary screening stage are not intended to function as strict universal suitability boundaries for mine tailings. Given the highly heterogeneous nature of mine tailings systems, the framework intentionally does not treat these criteria as definitive acceptance or rejection limits. Instead, they are used to support preliminary taxonomy-based grouping prior to the mineralogical evaluation stage, which constitutes the central interpretative component of the framework.

Tailings identified as requiring activation to enhance or unlock their reactivity are subsequently subjected to a mineralogical evaluation to establish their compatibility with specific treatment strategies. This involves determining the dominant mineral phases and their relative abundances, thereby defining the mineralogical basis for activation. On this basis, the tailings are evaluated against the proposed framework to identify the most appropriate activation pathway. Importantly, the framework evaluates tailings according to their existing chemical, physical, and mineralogical condition at the time of assessment, regardless of whether these characteristics originate from fresh processing conditions or prolonged environmental exposure and weathering.

Within the mechanical activation framework, minerals are classified according to two criteria: their functional contribution to the cementitious matrix and their activation response and structural susceptibility to mechanical breakdown. They are grouped into three main categories: Si–Al contributors (subdivided into energy-responsive and energy-intensive), oxide contributors (subdivided into carbonates-reactivity via calcination and low-reactivity oxides), and unsuitable phases (including sulfide-bearing minerals and structurally resistant minerals). This classification is grounded in intrinsic mineral attributes such as bond topology, structural connectivity, Mohs hardness, and cleavage, which collectively govern susceptibility to mechanical activation.

Finally, the activated tailings are evaluated for their functional contribution within cementitious matrices, thereby connecting initial taxonomy-based screening to targeted activation outcomes. By embedding mineralogical insights into activation pathways, the framework links raw material classification with likely functional behaviour and provides a basis for more systematic interpretation of mine-tailings valorisation.

In practical mine-tailings applications, the framework supports first-stage screening and interpretation using relatively accessible characterisation data. Bulk chemical composition provides an initial assessment of environmental constraints and overall oxide chemistry, including the presence of sulphur-bearing phases, potentially toxic elements, and the relative abundance of major oxides such as SiO_2, Al_2O_3, Fe_2O_3, CaO, and MgO. This preliminary screening stage enables differentiation between tailings potentially suitable for direct utilisation, those requiring activation-oriented assessment, and those potentially unsuitable because of environmental or compositional limitations. In this way, the framework allows preliminary differentiation of the general valorisation category and activation potential of the tailings before proceeding to mineralogical evaluation of activation behaviour. However, bulk chemistry alone is insufficient to evaluate activation potential, since chemically similar tailings may exhibit fundamentally different mechanochemical behaviour depending on their mineralogical assemblage. Consequently, modal mineralogical analysis represents the key interpretative stage of the framework, enabling differentiation between minerals potentially responsive to mechanical activation (e.g., layered aluminosilicates) and structurally resistant phases such as quartz or dense oxides. Particle-size distribution is incorporated as an additional engineering parameter related to grinding demand and processability, providing practical insight into the degree of comminution likely required prior to utilisation. In this way, the framework introduces a "mineralogical fingerprint" perspective that support preliminary grouping and prioritisation of tailings according to their likely activation behaviour and potential valorisation pathway before detailed laboratory-scale validation. Although detailed experimental validation remains necessary, this approach supports the preliminary identification of tailings with greater potential for specific valorisation pathways.

4. Mineralogical and mechanistic background

Mechanical activation represents a versatile pathway for enhancing the reactivity of mine tailings that would otherwise remain largely inert, by inducing structural disorder, increasing surface area, and altering particle morphology (Baláž, 2008). The application of mechanical energy through grinding or milling destabilises the crystal structure of minerals, disrupts long-range atomic order. This process can induce partial or complete amorphisation, generating phases with enhanced solubility and higher reactivity of oxides (SiO_2, Al_2O_3, Fe_2O_3, MgO) that can participate in cementitious hydration reactions (Baláž, 2008; Avvakumov et al., 2002; Boldyrev, 2006). Beyond structural changes, the process also reduces particle size and increases specific surface area (SSA), both of which accelerate dissolution kinetics and enhance reactivity even in minerals that resist amorphization (Baláž, 2008; Avvakumov et al., 2002). However, the response of mechanical activation is highly variable and depends largely on the structural and bonding characteristics of the dominant mineral phases, as well as the specific energy demand required to induce such transformations (Feng et al., 2024). Therefore, understanding the response of heterogeneous mine tailings to mechanical activation and to enhance its efficiency, it is essential to conduct assessments at the mineral level.

Mechanical activation is not a single-step phenomenon but a

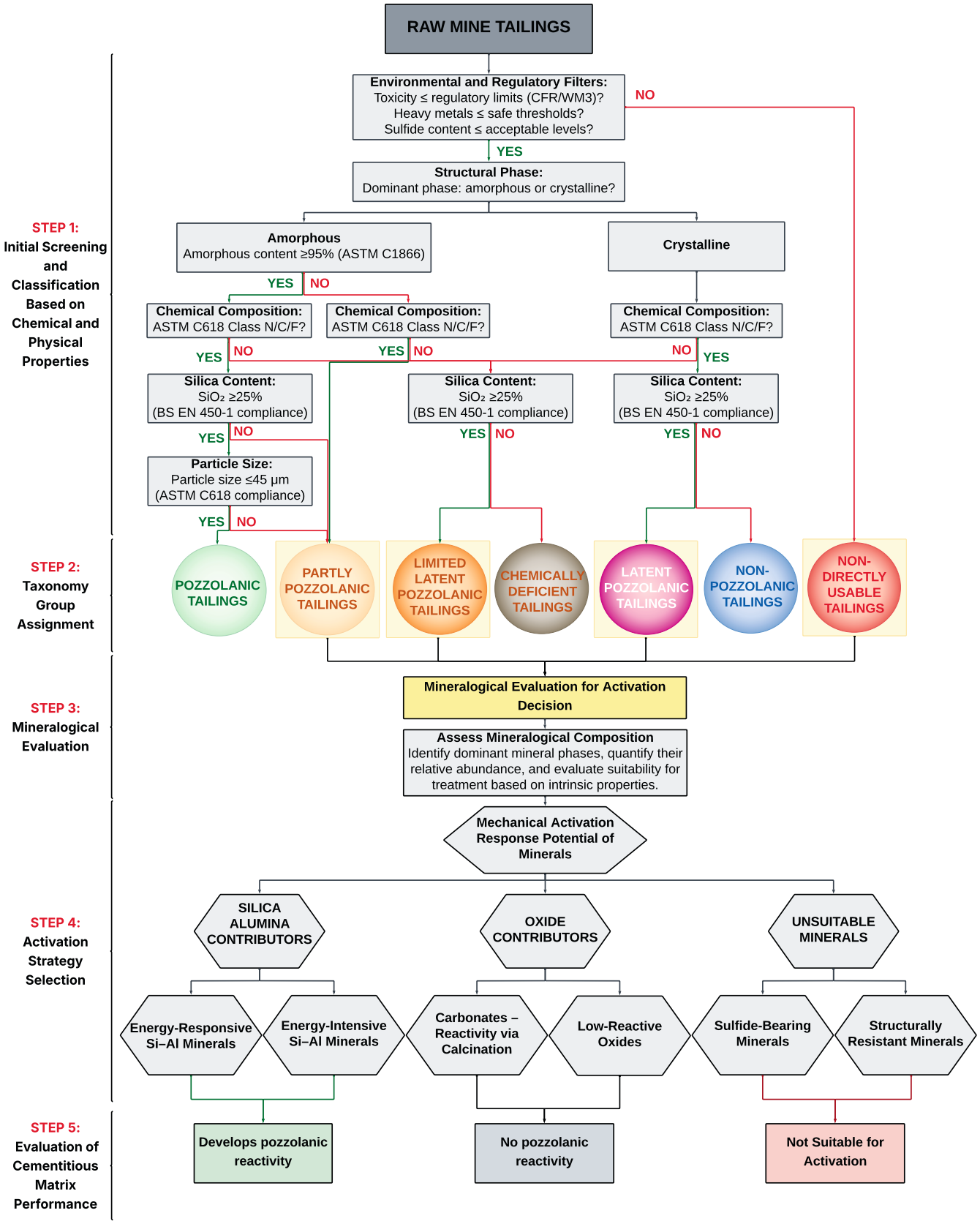

Fig. 2. Integrated framework for the classification and mechanical activation of mine tailings based on chemical, physical, and mineralogical characteristics. The framework incorporates preliminary screening criteria informed by Code of Federal Regulations (CFR), Waste Classification Technical Guidance WM3, ASTM C618, ASTM C1866, and BS EN 450–1 for the evaluation of supplementary cementitious materials (SCMs).

complex, multi-stage process. The input of mechanical energy induces lattice disorder, defect accumulation, and amorphization, while also increasing surface area and altering morphology. These structural and microstructural transformations evolve through sequential stages, whose predominance depends on the energy intensity and mineral structure. Consequently, the enhanced reactivity observed cannot be attributed to a single factor such as defect formation but arises from the interplay of multiple structural and process-related parameters (Baláž, 2008; Avvakumov et al., 2002; Boldyrev and Tkáčová, 2000). In literature, these transformations are collectively referred to as the mechanochemical response (Baláž, 2008; Juhász and Opoczky, 1990).

The parameters governing this response can be grouped into two categories: Processing parameters governing mechanical activation including; mill type, rotational speed, grinding duration, grinding mode, and atmospheric environment and intrinsic mineral attributes including; hardness, cleavage, bond topology, and structural connectivity. The following subsections examine these parameters individually, establishing the mineralogical foundation for the framework presented in this study.

4.1. Processing parameters governing mechanical activation

Structural transformations during mechanical activation are governed not only by the intrinsic crystal structure of minerals but also by milling parameters (e.g., mill type, rotational speed, grinding duration, grinding mode, and grinding media type) and environmental conditions (e.g., oxidising or reducing atmosphere, temperature, pH, and CO_2 availability) (Baláž, 2008). These parameters determine both the intensity and the mechanism of energy transfer to the mineral, directly influencing the interplay between particle fracture, defect accumulation, lattice distortion, amorphization, and agglomeration (Baláž, 2008; Boldyrev and Tkáčová, 2000). Although processing conditions may significantly influence the extent and efficiency of mechanochemical transformation, they modify rather than fundamentally redefine the intrinsic mineralogical activation tendency associated with different mineral systems.

Mill type dictates the dominant energy transfer mechanism, thus the mode of defect accumulation. Rotational speed and grinding duration control the energy input's intensity and continuity; however, exceeding the optimal duration can trigger particle re-agglomeration (Baláž, 2008). Grinding mode also alters outcomes; dry grinding typically induces higher lattice strain and crystal distortion, while wet grinding, though less structurally disruptive, often promotes greater increases in surface area. This is largely due to the dissolution of alkali ions in the liquid phase, which raises the pH and accelerates mineral dissolution and reprecipitation processes (Avvakumov et al., 2002). Atmospheric conditions are equally critical. Inert environments mainly facilitate defect formation, while oxygen enables oxidative phase transformations (Avvakumov et al., 2002; Pourghahramani and Akhgar, 2015). Additionally, initial particle size and grinding time critically affect surface area development and the threshold for agglomeration (Pourghahramani, 2006). Specific surface area increases rapidly during initial grinding due to particle fracture, but prolonged milling promotes re-coalescence of high-energy particles through van der Waals and electrostatic interactions, ultimately reducing effective surface area (Baláž, 2008; Juhász and Opoczky, 1990).

These mechanisms are clearly reflected in the literature. For hematite ground for nine hours, a planetary ball mill achieved ~ 85% amorphisation and significant lattice strain while a vibratory mill produced only 58–60%, and a tumbling mill reached ~ 70% despite lower surface area gains (Pourghahramani, 2006). These outcomes reflect the energy transfer characteristics of each mill: planetary mills generate high rotational speeds and strong impact–shear forces, vibratory mills deliver lower energy impacts with limited shear, and tumbling mills, though low in impact energy, promote defect accumulation through prolonged friction (Baláž, 2008; Pourghahramani, 2006). In ilmenite, rotational speed and grinding mode were decisive; amorphisation advanced slowly at 300 rpm but was accelerated at 450 rpm (Wei et al., 2009). Moreover, dry grinding achieved 95% amorphisation within 150 min, compared with 69% under wet conditions, although the alkalisation of the wet medium increased dissolution rates and intensified surface reactions (Ebadi and Pourghahramani, 2019). Similar trends were reported for pyrite, where grinding under argon increased defect density, while milling in air induced oxidative secondary phases (Pourghahramani and Akhgar, 2015). Re-agglomeration tendencies have been reported in long-term grinding of hematite, where prolonged energy input eventually promotes particle coalescence despite initial surface area gains (Pourghahramani, 2006). In gibbsite, the specific surface area rose from 1.4 to 70.36 m^2/g within 180 min but declined to 57.63 m^2/g after 240 min due to re-agglomeration, sintering under moist conditions and the collapse of mesopores smaller than 16 nm (Alex et al., 2014).

To sum up, processing parameters are not merely supportive conditions but decisive, interdependent variables in mechanical activation. Mill type, speed, mode, atmosphere, and duration collectively govern the dynamic balance between fragmentation, defect accumulation, amorphisation, and agglomeration. Even for the same mineral, variations in these parameters can yield markedly different structural outcomes. This variability highlights a gap in the systematic optimisation of processing conditions and underscores the need to treat milling parameters not as constant but as critical design variables that can be systematically adjusted to enhance reactivity while minimising unwanted effects such as over-agglomeration or energy inefficiency.

4.2. Intrinsic mineral attributes governing mechanical activation

4.2.1. Mohs hardness and cleavage

In addition to milling parameters, intrinsic physical properties of minerals strongly influence their response to mechanical activation. Among these, hardness and cleavage act as key modifiers of effective energy demand by controlling resistance to stress and the efficiency of stress propagation along weak planes (Juhász and Opoczky, 1990; Deer et al., 2013). Mohs hardness provides a relative measure of resistance to scratching or indentation and reflects the force required to initiate disruption of atomic bonds (Deer et al., 2013) whereas cleavage describes the tendency of a mineral to split along crystallographic planes of weakness; in minerals lacking cleavage, fracture governs irregular breakage (Deer et al., 2013). Together, these properties determine how mechanical energy is absorbed, transmitted, and dissipated within a mineral lattice (Juhász and Opoczky, 1990; Deer et al., 2013).

Mohs hardness, ranging from 1 (talc) to 10 (diamond), provides only a relative scale of softness and hardness, as the increments between integers are non-linear. For example, the indentation resistance between quartz (7) and corundum (9) is far greater than that between calcite (3) and fluorite (4) (Deer et al., 2013). Absolute hardness measurements, such as Vickers or Knoop tests, quantify indentation resistance in GPa (Baláž, 2008; Juhász and Opoczky, 1990; Deer et al., 2013), but Mohs hardness still broadly correlates with bond strength and the force required for lattice disruption. In mechanical activation, low-hardness minerals accumulate defects and disorder at relatively low milling intensities, whereas high-hardness minerals mainly dissipate energy through brittle fracture and microcracking, limiting amorphisation (Baláž, 2008; Juhász and Opoczky, 1990).

Cleavage further modifies this response. Minerals with perfect cleavage (e.g., micas, halite, calcite) split smoothly along defined planes, enabling efficient stress propagation and lowering the energy input required for particle reduction (Deer et al., 2013). Minerals with imperfect cleavage (e.g., feldspars, amphiboles) require greater energy input and exhibit mixed cleavage–fracture behaviour. Non-cleavable minerals (e.g., quartz, olivine) resist splitting entirely; applied stress is dissipated by conchoidal fracture, an energetically costly process (Deer et al., 2013). For example, quartz shows conchoidal fracture with curved

shell-like surfaces, reflecting both its high hardness and resistance to lattice collapse (Baláž, 2008). The energy required to cause cleavage will also be influenced by factors such as the presence of defects, microcracks, and grain boundaries. Fig. 3 illustrates the effect of hardness and cleavage on the mechanical activation behaviour of minerals.

In summary, hardness defines the baseline resistance of a lattice to applied stress, while cleavage governs the efficiency of stress release along weak planes. Minerals with low hardness and perfect cleavage (e.g., micas, calcite) undergo rapid disruption at low energy input, whereas hard, non-cleavable minerals (e.g., quartz, olivine) demand high energies that are mostly consumed in fracture rather than amorphisation. These attributes therefore define the mineral-specific energy thresholds that critically shape mechanochemical response and underpin activation outcomes.

4.2.2. *Bond topology and structural connectivity*

Although processing parameters such as mill type, powder-to-ball ratio, and milling environment, together with intrinsic physical properties like hardness and cleavage, influence the extent of structural change during mechanical activation, the decisive control lies in crystallographic attributes, specifically bond topology and structural connectivity (Baláž, 2008; Juhász and Opoczky, 1990; Butyagin, 1994). Other factors, including atomic packing density (notably in non-silicates) and the lattice's ability to accommodate defects, may modulate behaviour, but it is topology and connectivity that ultimately determine whether a structure delaminates, disorders, amorphises, or merely accumulates defects (Baláž, 2008; Avvakumov et al., 2002; Juhász and Opoczky, 1990). These attributes govern weak planes, interlayer forces, and three-dimensional cross-linking, thus defining the mechanochemical response (Juhász and Opoczky, 1990).

Bond topology refers to the arrangement of structural units within a mineral (Deer et al., 2013). In contrast, structural connectivity describes the density and strength of bonds, including interlayer interactions and polyhedral compactness (Deer et al., 2013). Together, these attributes account for the diverse mechanochemical responses of minerals; some structures amorphise readily, while others resist collapse and accommodate stress through defect formation.

In general, minerals are divided into silicates and non-silicates (Deer et al., 2013). Silicate minerals are further classified into six groups based on the degree of polymerization of SiO_4 tetrahedra; nesosilicates (isolated tetrahedra), sorosilicates (double tetrahedra), cyclosilicates (ring structures), inosilicates (single and double chains), phyllosilicates (sheet structures), and tectosilicates (three-dimensional frameworks) (Deer et al., 2013). Phyllosilicates (e.g., talc, kaolinite, muscovite) consist of

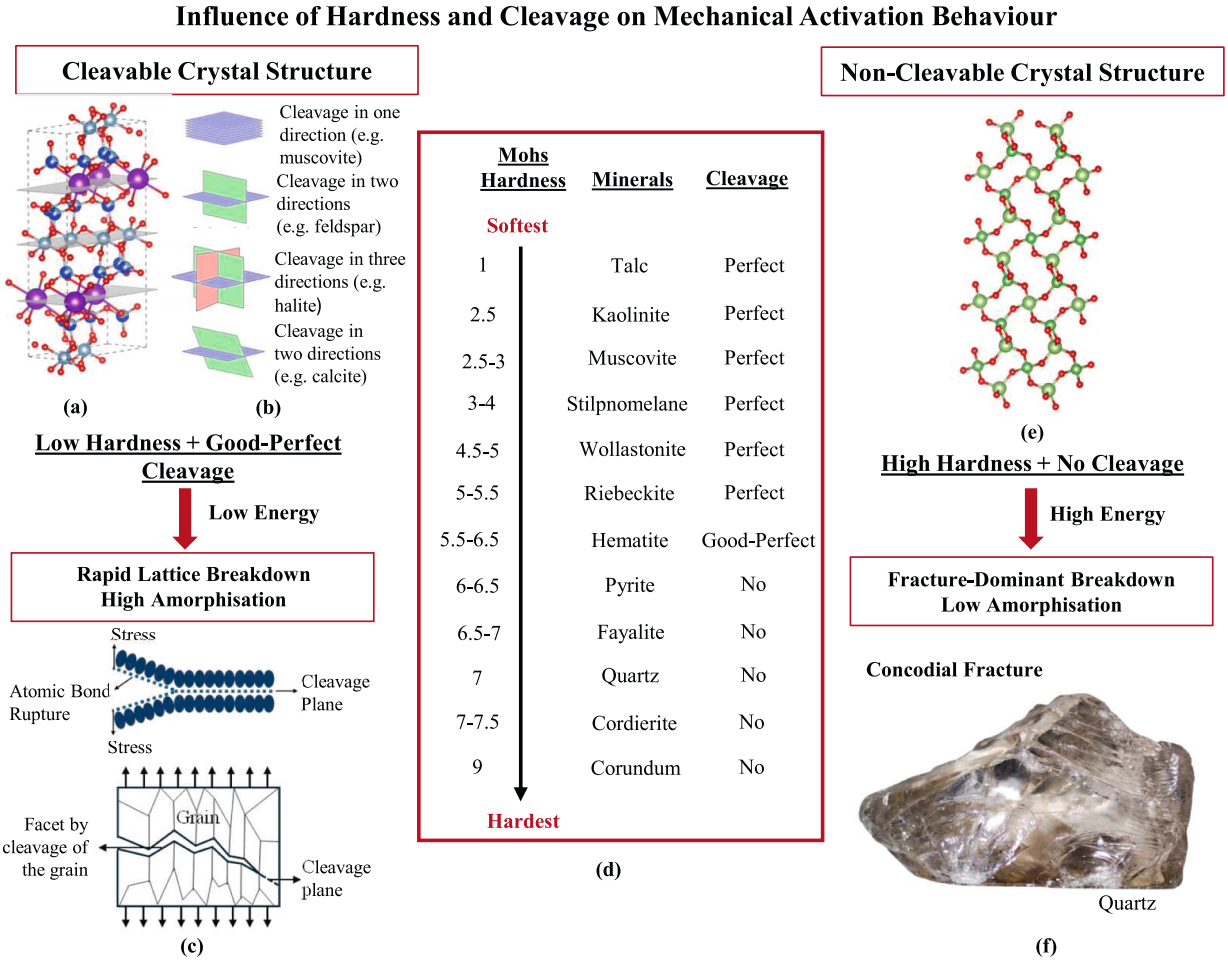

Fig. 3. Effect of mineral hardness and cleavage on mechanical activation behaviour. (a) Layered crystal structure of muscovite illustrating basal cleavage planes parallel to the (001) crystallographic direction, visualised using VESTA software (Momma and Izumi, 2011). (b) Schematic representation of mineral cleavage types based on the number and orientation of cleavage planes, adapted from Rygel (Rygel, 2010), via Wikimedia Commons, licensed under Creative Commons Attribution–ShareAlike 3.0 (CC BY-SA 3.0). (c) Schematic illustration of cleavage fracture propagation across polycrystalline grains, showing the formation of cleavage facets within individual grains under tensile stress, based on concepts described in González-Velázquez (González-Velázquez, 2018). (d) Mohs hardness scale and cleavage properties of representative minerals, compiled from (Mindat.org. (n.d.). Mindat mineral database. Retrieved August 2, 2025). (e) Three-dimensional framework structure of quartz illustrating the absence of preferred cleavage planes, visualised using VESTA software (Momma and Izumi, 2011). (f) Conchoidal fracture observed in quartz. Photograph adapted from St. John (St. John, J., 2021), licensed under Creative Commons Attribution 2.0 (CC BY 2.0).

two-dimensional layers with weak interlayer bonding, rendering them highly susceptible to delamination and amorphisation (Juhász and Opoczky, 1990). Inosilicates form chain-like tetrahedral arrangements (single-chain pyroxenes, double-chain amphiboles) with stronger bonding (Baláž, 2008; Juhász and Opoczky, 1990). Sorosilicates show limited disorder, mainly dissipating energy through fracture (Juhász and Opoczky, 1990), while cyclosilicates form stable ring frameworks with moderate to high resistance (Deer et al., 2013). Nesosilicates, though isolated, are stabilised by dense cation coordination (e.g., olivine, garnet), limiting lattice degradation (Baláž, 2008; Juhász and Opoczky, 1990). Tectosilicates (quartz, feldspars) have fully interconnected frameworks that absorb energy mostly by fracture rather than amorphisation (Baláž, 2008; Juhász and Opoczky, 1990). Fig. 4 illustrates the structural classification of silicate minerals and their relative susceptibility to mechanical activation as governed by SiO_4 tetrahedral connectivity and framework rigidity.

However, non-silicate minerals further expand this structural hierarchy with distinct topological motifs. Carbonates comprise planar CO_3 groups linked by cations and usually fragment/develop defects under milling; amorphisation is rare without calcination (Deer et al., 2013). Oxides and hydroxides adopt dense O^{2-}/OH^{-} packing (e.g., rutile, spinel, corundum), strongly resisting collapse (Deer et al., 2013). Sulfides, structurally analogous but less covalent, may undergo surface oxidation and form secondary phases depending on milling atmosphere and duration (Deer et al., 2013). Corundum exemplifies the upper bound of structural resistance (Deer et al., 2013).

Bond topology (e.g., sheet, chain, framework) provides only a general tendency; layered structures amorphise more readily, whereas three-dimensional frameworks are generally more resistant (Baláž, 2008; Avvakumov et al., 2002; Juhász and Opoczky, 1990). However, mechanochemical processability also depends on structural connectivity, density of linkages, bridging configurations, cation type, and void filling. As emphasized by Baláž (2008) (Baláž, 2008) and Juhász and Opoczky (1990) (Juhász and Opoczky, 1990), even minerals within the same topological class can exhibit markedly different mechanochemical responses. For instance, albite (a tectosilicate) amorphises more easily than quartz owing to Na^{+} and Al–Si disorder, while epidote (a sorosilicate) resists collapse due to compact Al–O linkages (Baláž, 2008). Similarly, though all phyllosilicates are layered, interlayer bonding differs (Deer et al., 2013). Talc is disrupted by van der Waals forces, kaolinite is stabilised by hydrogen bonds, and montmorillonite shows complex behaviour due to exchangeable cations and interlayer water By contrast, illite and micas (muscovite, biotite) resist activation because of strong K^{+} interlayers (Avvakumov et al., 2002; Juhász and Opoczky, 1990; Deer et al., 2013). In inosilicates, cross-linking by $Ca2^{+}$ and $Mg2^{+}$ strengthens chains, so pyroxenes and amphiboles mainly accumulate defects rather than collapse (Juhász and Opoczky, 1990; Deer et al., 2013). On the other hand, carbonates, built from planar CO_3^{2-} groups stacked by ionic bonds, typically fragment under stress, developing defects rather than fully amorphising; calcination is usually required (Baláž, 2008; Avvakumov et al., 2002; Juhász and Opoczky, 1990). Nesosilicates like olivine and garnet, though isolated tetrahedra, are

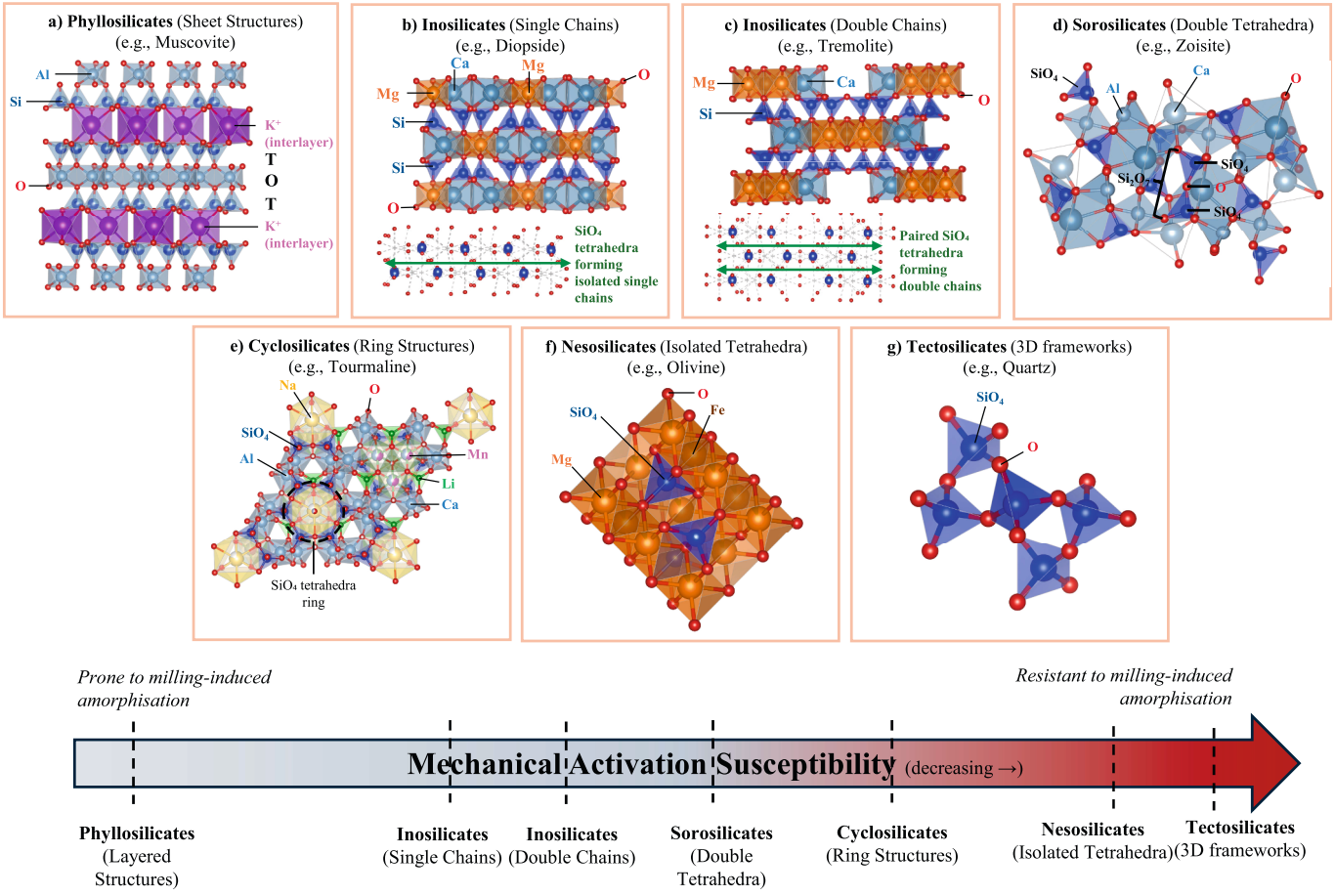

Fig. 4. Atomic structures of representative silicate minerals classified according to SiO_4 tetrahedral connectivity: (a) phyllosilicates (e.g., muscovite), (b–c) inosilicates with single and double chains (e.g., diopside; tremolite), (d) sorosilicates (e.g., zoisite), (e) cyclosilicates (e.g., tourmaline), (f) nesosilicates (e.g., olivine), and (g) tectosilicates (e.g., quartz). The arrangement reflects decreasing susceptibility of these structures to milling-induced amorphisation from left to right. Atomic structures were visualised using VESTA software (Momma and Izumi, 2011); mineral classification and examples follow the mineralogy rein (Source OpenGeology.org. (n.d.). , 2025).

stabilised by dense cation coordination (Fe^{2+}, $Mg2^{+}$, $Ca2^{+}$), so energy is consumed in cracking and defect formation with minimal amorphization. (Deer et al., 2013). Fayalite may show increased solubility under high-energy milling in alkaline media, but not full amorphisation (Juhász and Opoczky, 1990). Oxides and sulfides, with dense packing and strong bonds, resist strongly; energy input produces defects and cracks rather than collapse. In sulfides, milling can cause surface oxidation and generate secondary phases such as elemental sulfur, sulfates, or oxides depending on atmosphere and duration (Baláž, 2008). Corundum exemplifies the highest resistance, with O^{2-} ions close-packed and $Al3^{+}$ filling all octahedral sites (Deer et al., 2013).

In summary, considering topology and connectivity together reveals fundamental insights in mechanochemical resistance. Layered silicates with weak interlayers (e.g., talc, swelling smectites) are the most susceptible. Kaolinite, stabilised by hydrogen bonding, shows somewhat greater resistance, while illitic and muscovitic/biotitic phyllosilicates with K^{+} interlayers are progressively more stable within the phyllosilicate family. Beyond phyllosilicates, chain silicates exhibit higher robustness through Ca^{2+} and Mg^{2+} cross-links. At a comparable or slightly higher level, carbonates generally fragment and develop defects rather than amorphise. Framework silicates (quartz, feldspars) and nesosilicates (olivine, garnet) show substantially greater resistance, while oxides and sulfides with dense ionic or covalent packing represent the upper bound, with corundum at the extreme. Although these patterns derive from pure mineral phases, exceptions remain, and actual behaviour depends strongly on mineralogical context and processing conditions.

Collectively, bond topology and structural connectivity explain why some minerals collapse under milling while others resist, defining the limits of mechanochemical response. Ultimately, whether mechanical activation yields amorphisation or merely defect accumulation reflects the interplay of crystallography with processing conditions. The integration of these dimensions provides the mineralogical foundation of the activation framework, showing that heterogeneous tailings must be understood as mineral assemblages whose dominant phases play a primary role in governing collective behaviour. This integrated perspective offers a systematic and mechanistically informed basis for the valorisation of mine tailings and supports sustainable binder design.

5. Results and discussion

5.1. Mineral-based mechanical activation framework

Mine tailings typically consist of heterogeneous mineral assemblages in which multiple phases coexist and interact during mechanical processing. In such systems, mineral–mineral interactions may influence fracture propagation, energy dissipation during milling, amorphisation behaviour, and dissolution processes (Baláž, 2008). Consequently, understanding the intrinsic activation response of the constituent mineral phases provides a fundamental basis for interpreting the behaviour of heterogeneous tailings systems. Within this context, a mineral-based mechanical activation framework (Fig. 5) was developed to classify common minerals in mine tailings according to two criteria: their potential contribution to cementitious matrices and their susceptibility to

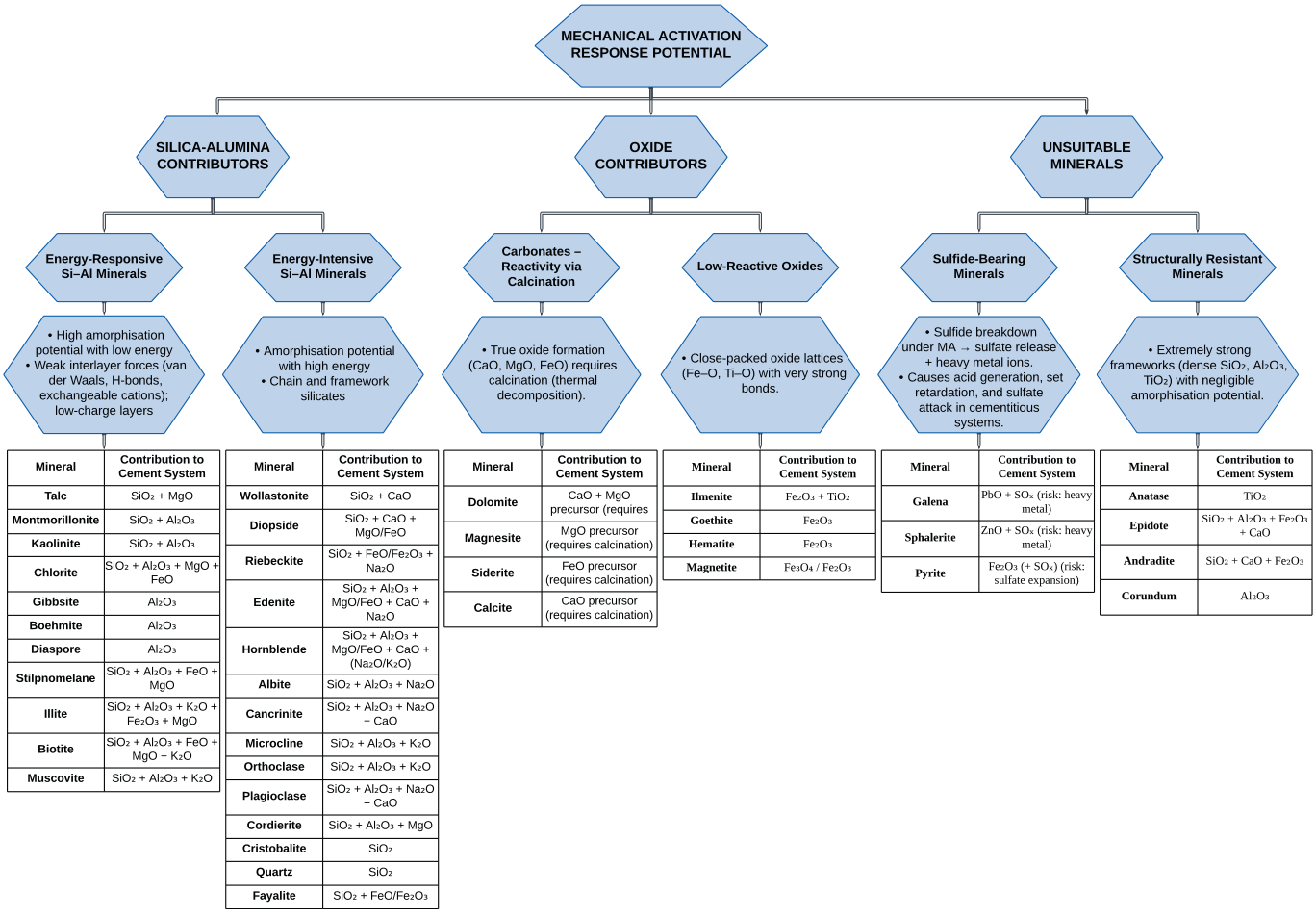

Fig. 5. Mineral-based mechanical activation framework classifying mine-tailings minerals based on Mohs hardness, cleavage characteristics, and their potential contribution to cementitious systems. The mineral groups and representative phases illustrated reflect mineralogical constituents widely reported across mine tailings literature. The framework is conceptualised and designed by the authors.

structural breakdown.

Specifically, the framework first differentiates minerals by the type of products they can yield in cementitious systems upon amorphization such as reactive silica and alumina, metal oxides, or potentially deleterious sulfide-derived phases. It then ranks them internally according to degree of transformation and the energy required under milling. By integrating reactive contribution and amorphisation potential, the framework seeks to identify the minerals most effective within cementitious matrices, thereby opening a pathway for interpreting and enhancing the performance of mine tailings under mechanical activation. The mineral groups and representative phases considered in this framework reflect mineralogical constituents widely reported in mine tailings literature and are selected to represent the dominant mechanical activation response patterns relevant to cementitious applications.

The first category, "Silica–Alumina Contributors", contains minerals rich in silica and/or alumina that can transform into reactive forms and promote calcium silicate hydrate (C–S–H) and calcium aluminosilicate hydrate (C–A–S–H) formation. This group is divided into subgroups according to energy demand. The first subgroup, "Energy-Responsive Si–Al Contributors", includes phyllosilicates and aluminium hydroxides/oxyhydroxides, all characterised by weakly bonded, low-connectivity frameworks. Aluminium hydroxides such as gibbsite, boehmite, and diaspore act primarily as alumina sources, whereas silicate minerals such as kaolinite, talc, and montmorillonite provide reactive silica upon breakdown. From a mechanical perspective, these minerals typically exhibit low hardness values (Mohs 1–2.5) and perfect cleavage, features that facilitate delamination and disordering under milling. Reactivity spans from highly responsive talc to more resistant muscovite. The second subgroup, "Energy-Intensive Si–Al Contributors", can also provide reactive silica and/or alumina but exhibits stronger crystal frameworks that demand higher milling energy. Typical members include chain silicates such as wollastonite and diopside, which are moderately responsive, and more rigid amphiboles with stronger bonding. At the most resistant end are feldspars and quartz, whose fully polymerised three-dimensional frameworks hinder amorphisation, while fayalite remains largely inert under dry milling but may respond under wet or alkaline conditions. These minerals generally fall within the mid-to-high Mohs hardness range (5–7) and exhibit limited cleavage, features that reflect their greater resistance and the higher energy demand required for effective activation.

The second main group, "Oxide Contributors", includes minerals that yield reactive oxides when structurally deformed. It is divided into two subgroups. The first, "Carbonates – Reactivity via Calcination", comprises minerals such as calcite and dolomite, show limited mechanochemical response because of their dense carbonate lattices. Milling may induce minor defect formation but does not liberate CO_2. True reactivity only develops after calcination, which produces highly reactive oxides such as CaO, MgO, or FeO. The second subgroup, Low-Reactive Oxides, includes iron- and titanium-bearing minerals such as hematite, magnetite, ilmenite, and goethite. Their close-packed lattices confer low amorphisation potential; when they do respond to mechanical activation, the transformation pathway predominantly generates/exposes Fe-oxide/Ti-oxide phases (e.g., Fe_2O_3, Fe_3O_4, TiO_2). Among these, ilmenite and goethite are relatively more defect-prone and show greater Fe-oxide release under milling, while hematite and magnetite exhibit the highest lattice persistence.

The third main group, "Unsuitable Minerals", comprises phases that either generate harmful by-products or resist structural breakdown to such an extent that they cannot be valorised by mechanical activation. Two subgroups are distinguished. The first subgroup, "Sulfide-Bearing Minerals" (e.g., pyrite, galena, sphalerite), are mechanically unstable yet chemically problematic: while their lattices fracture easily under milling, this process releases sulphates and heavy metals (Pb, Zn, Fe) that severely compromise cementitious performance. Although their metallic bonding frameworks readily collapse under impact, the resulting products are detrimental to both durability and environmental safety. The second subgroup, "Structurally Resistant Minerals", includes phases such as corundum (Al_2O_3), anatase (TiO_2), epidote, and andradite. Their tightly bonded three-dimensional networks, dominated by strong ionic or covalent linkages, confer very high hardness (Mohs 6–9) and minimal or no cleavage, making them resistant to delamination or disordering. Even under intensive milling, these frameworks remain largely intact, preventing meaningful amorphisation. Despite containing potentially useful elements such as Si, Al, or Ti, their rigid crystal lattices lock these components in inaccessible forms, rendering the minerals unsuitable for cementitious utilisation.

To sum up, the mineral-based mechanical activation framework reframes tailings valorisation as a more systematic and mineralogically informed approach rather than a purely empirical practice. By jointly considering cementitious contribution and amorphisation potential, it identifies when milling alone is appropriate (energy-responsive phyllosilicates and Al-hydroxides), when complementary routes are required (energy-intensive silicates and carbonates that become reactive only after calcination), and when materials should be excluded on durability or environmental grounds (sulfide-bearing and structurally resistant phases). Grouping minerals into energy-responsive and energy-intensive categories also enables a relative energy budgeting approach, allowing practitioners to anticipate whether simple milling suffices or whether complementary treatments are required. Operationally, the framework can be implemented using routine characterisation (XRD and X-ray fluorescence (XRF), together with hardness and cleavage proxies) to triage heterogeneous tailings into process pathways and inform binder design.

5.2. Mineral-specific response to mechanical Activation: Crystallographic and energetic considerations

While the framework outlined above establishes a mechanistically informed basis for interpreting the behaviour of heterogeneous tailings, its validity ultimately depends on the response of individual minerals under actual milling conditions. Mine tailings are mineral assemblages, and the overall reactivity of the system is dictated by the crystallographic and energetic characteristics of the dominant phases. In heterogeneous systems, interactions among coexisting mineral phases may also influence the activation behaviour. This section therefore verifies the framework by examining mineral-specific behaviours reported in the literature, with particular attention to how structural topology, bonding strength, Mohs hardness, and cleavage influence amorphisation pathways. By analysing representative studies across the main mineral groups, Si–Al contributors, oxide contributors, and unsuitable phases, the proposed categories introduced in Section 5.1 are evaluated against empirical evidence. It is also evident that milling parameters exert a decisive influence on mineral responses. Comparative studies on the same mineral, conducted under varying milling times, intensities, and media, have reported markedly different degrees of amorphisation and reactivity. The multi-mineral datasets summarised in the accompanying tables demonstrate that the observed variability stems from differences in experimental conditions rather than from fundamental discrepancies in mineral behaviour. Accordingly, milling parameters have been explicitly incorporated into both the tables and the discussion in this section, ensuring that mineral behaviour is interpreted considering process conditions as well as intrinsic crystallographic attributes. The aim is to refine the classification, identify mineral-specific exceptions, and establish a mechanistic foundation for linking crystallography with cementitious matrix reactivity.

5.2.1. Silica-Alumina Contributors

The group of Silica–Alumina Contributors comprises minerals containing silica and/or alumina that are capable of generating reactive phases through amorphisation under milling. Within this category, two subgroups can be distinguished: energy-responsive phases, which undergo rapid disordering under low-intensity milling, and energy-

intensive phases, which require substantially higher energy input owing to the rigidity of their crystal frameworks. Table 1 summarises representative studies of these minerals, including structural characteristics, milling parameters, amorphisation behaviour, and cementitious contributions.

The energy-responsive Si-Al minerals group comprises phyllosilicates and aluminium hydroxides/oxyhydroxides, which are characterised by layered or sheet-like architectures with interlayer interactions ranging from van der Waals forces and exchangeable cations to hydrogen bonding and, in some cases, K^+-bridged 2:1 layers of higher rigidity (Deer et al., 2013). Functionally, the amorphous domains generated from these structures serve as accessible sources of reactive silica and alumina. Representative studies highlight the mechanistic role of structural topology, cleavage quality, and bond strength in determining activation. Talc (Mohs 1), with weak van der Waals interlayers, undergoes pronounced amorphisation after only 30 min of ultra-centrifugal milling, yielding metastable amorphous silica (Andrić et al., 2014). Kaolinite, with a hydrogen-bonded 1:1 layered framework, has been found to require ~ 60 min of planetary milling to induce substantial structural disorder; nevertheless, the activated phase has exhibited high pozzolanic performance, with strength activity indices exceeding 90% (Baki et al., 2022).

Aluminium hydroxides have been reported to respond efficiently to mechanical activation. Gibbsite (Mohs 2.5–3), with perfect cleavage and hydrogen-bonded layers, has reached ~ 95% amorphisation after 240 min of milling, accompanied by Al–OH bond breakdown and increased dissolution; the disordered phase has been identified as a source of reactive alumina (Alex et al., 2014). Muscovite, although representing the upper resistance boundary of this subgroup due to strong K^+ bridges and high structural connectivity, has nevertheless shown reduced crystallinity (~15% after 160 min) and significant dehydroxylation, with the resulting phases consuming portlandite and forming C–A–S–H gels (Baki et al., 2022; Yao et al., 2019).

Energy-intensive Si–Al minerals include chain silicates and framework silicates, which have been reported to require substantially greater milling intensities due to their rigid crystal structures. Among these, wollastonite and diopside are comparatively easier to activate owing to their single-chain connectivity, whereas feldspars and quartz represent the opposite extreme with highly polymerised three-dimensional frameworks (Juhász and Opoczky, 1990; Deer et al., 2013). Fayalite, a Fe-rich olivine, shows comparable resistance under dry milling but has been reported to partially disorder in wet or alkaline environments (Juhász and Opoczky, 1990; Deer et al., 2013).

Wollastonite (Mohs 4.5–5, Ca–O bonds) and diopside (Mohs 5.5–6.5, Mg–O bonds), both single-chain inosilicates, have been reported to undergo near-complete amorphisation under prolonged low-energy milling (100 rpm), requiring approximately 317 h and 512 h, respectively (Murouchi et al., 2021). These phases have nevertheless yielded reactive silica and released Ca and Mg species, which have been shown to contribute to cementitious hydration (Murouchi et al., 2021). Feldspars have displayed variable reactivity depending on framework distortion. Microcline (Mohs 6–6.5) has been reported to undergo near-complete amorphisation within ~ 120 min of planetary milling, facilitated by weaker Si–O–Al linkages and structural distortions introduced by Al substitution and K^+ interstitials (Alyosif et al., 2023). Albite has shown extensive amorphisation within ~ 90 min under similar conditions, yielding reactive silica, alumina, and Na (Alyosif et al., 2023). These activated feldspars have been observed to contribute reactive silica and alumina, though generally with lower efficiency than phyllosilicates. Quartz (Mohs 7, 3D Si–O–Si network) has consistently been reported as the most resistant mineral. Limited disorder has been observed only after ~ 300 min of milling at 500 rpm, while near-complete amorphisation has been achieved within 60 min at 800 rpm, though often accompanied by contamination from the milling media (Gobindlal et al., 2021; Kweon et al., 2025). Activated quartz has primarily contributed surface-derived reactive silica rather than bulk transformation, aligning with its framework classification.

Fayalite (Fe-rich nesosilicate, Mohs 6.5–7, no cleavage, isolated SiO_4 tetrahedra linked by Fe^{2+}) has been shown to exhibit strongly condition-dependent behaviour. During dry milling, activation has generally been limited: even after extended grinding, studies have observed only partial disordering, with structural robustness maintained due to particle agglomeration, localized heating, and the absence of a reactive medium (Baláž et al., 2008; Šepelák et al., 2012). By contrast, wet and alkaline milling have repeatedly been reported to accelerate breakdown through hydroxide-induced cleavage of Fe–O and Si–O bonds, releasing $Fe2^+$ and silicate (Šepelák et al., 2012). For example, Planetary dry milling at 450 rpm has produced ~ 83% amorphisation within 30 min (Baláž et al., 2008), while attritor milling under wet conditions yielded ~ 88% after 120 min (Baláž et al., 2008). Nutating milling experiments have further demonstrated the role of water: ~43% disorder was observed after 10 min under dry conditions, whereas the introduction of water triggered rapid amorphisation in the same timeframe (Nadirov and Mussapyrova, 2020). Although different milling systems impart varying levels of specific energy, direct comparison is challenging due to limited quantitative energy data (e.g., kWh/kg). Nevertheless, the extent of amorphisation suggests that a critical energy threshold must be exceeded to initiate Fe–O and Si–O bond breakage. These transformations have been consistently associated with portlandite consumption and secondary C–S–H formation, confirming fayalite as an energy-intensive but environmentally responsive phase (Baláž et al., 2008; Šepelák et al., 2012; Nadirov and Mussapyrova, 2020).

In summary, phyllosilicates and hydroxides with weak interlayer bonds have been consistently shown to undergo rapid amorphisation and to enhance pozzolanic reactivity via portlandite consumption and C–S–H/C–A–S–H formation. In contrast, chain silicates, feldspars, and quartz have demonstrated the need for substantially higher milling intensities, while fayalite has highlighted the accelerating influence of wet and alkaline environments. Together, these results confirm the mechanistic link between crystallographic attributes, energy demand, and pozzolanic activation, providing a robust empirical basis for the subgrouping of Si–Al contributors.

5.2.2. Oxide-Contributors

The second group, defined as Oxide Contributors, consists of minerals whose reactivity derives from their ability to generate CaO, MgO, or FeO once structurally destabilised. Two subcategories can be distinguished: “Carbonates–Reactivity via Calcination”, whose reactivity emerges only after thermal decomposition and “Low-Reactive Oxides”, comprising dense Fe- and Ti-bearing oxides that exhibit strong resistance to amorphisation. Representative studies on minerals from both subgroups are summarised in Table 2.

Within the carbonates–reactivity via calcination subgroup, minerals such as calcite, dolomite, magnesite, and siderite have consistently been reported to resist oxide formation during milling, reflecting the stability of their CO_3^{2-} frameworks. For example, calcite (Mohs 3) shows only minor crystallinity loss during short-duration milling (e.g., ~4% reduction at 250–550 rpm), and although defect accumulation and partial polymorphic transformation to aragonite have been observed under extended high-energy milling, no reactive CaO is produced in the absence of calcination (Pesenti et al., 2008; Bańkowska-Sobczak et al., 2024). Thermal activation of calcite, on the other hand, has been shown to cause CO_2 release and the formation of reactive CaO as the primary oxide phase (Ban et al., 2021; Jiménez et al., 2022). Dolomite (Mohs 3.5–4) has shown pronounced lattice distortion under high-intensity milling (1820 rpm, 2 h), yet no CaO or MgO was generated (Kristóf and Juhász, 1993). Under thermal conditions, decomposition of dolomite has been reported to result in CO_2 release, yielding CaO and MgO as the final reactive oxide products (Olszak-Humienik and Jabłoński, 2015). Similar behavior has been reported for magnesite and siderite, where milling produced only micro strain or limited disorder (Olszak-Humienik and Jabłoński, 2015; Zuo et al., 2024), while calcination

Table 1
Summary of representative studies on minerals classified as "Silica–Alumina Contributors" within the proposed mechanical activation framework, including crystallographic characteristics, milling conditions, degree of amorphisation, and contribution to cementitious systems. Abbreviations: Si–Al, silica–alumina; C–S–H, calcium silicate hydrate; BPR, ball-to-powder ratio; rpm, revolutions per minute.

Ref	Mineral	Proposed Classification	Amorphization Potential Factors		Energy Requirement Factors		Milling Duration	Milling Conditions	Degree of Structural Distruption	Contribution to Cement Systems
			Bond Topology	**Structural Connectivity**	**Mohs Hardness**	**Cleavage Quality**				
(Andrić et al., 2014)	Talc	Energy-Responsive Si-Al Contributors	Layered Silicates	Van der Waals interlayers	1	Perfect	30 min	Ultra-centrifugal milling (Retsch ZM-1, 10,000–20,000 rpm, high-intensity, dry milling)	Extensive amorphisation (strong loss of crystallinity)	Reactive silica (SiO_2)
(Baki et al., 2022)	Montmorillonite	Energy-Responsive Si-Al Contributors	Layered Silicates	Exchangeable cation + H_2O interlayers	1–2	Perfect	40–60 min	Planetary ball milling (500 rpm, high-energy, dry milling)	Extensive amorphisation (strong loss of crystallinity)	Reactive silica (SiO_2) and alumine (Al_2O_3)
(Baki et al., 2022)	Kaolinite	Energy-Responsive Si-Al Contributors	Layered Silicates	H-bonded interlayers	2–2.5	Perfect	60 min	Planetary ball milling (500 rpm, high-energy, dry milling)	Extensive amorphisation (strong loss of crystallinity)	Reactive silica (SiO_2) and alumina (Al_2O_3)
(Alex et al., 2014)	Gibbsite	Energy-Responsive Si-Al Contributors	Non-silicate (Al-oxyhydroxide)	H-bonded layers	2.5–3	Perfect	240 min	Planetary milling (400 rpm, high-energy, dry milling)	~95% amorphisation (loss of crystallinity, OH bond breaking, structural water release)	Reactive alumina (Al_2O_3)
(Alex et al., 2014)	Boehmite	Energy-Responsive Si-Al Contributors	Non-silicate (Al-oxyhydroxide)	H-bonded layers	3–4	Perfect	240 min	Planetary milling (400 rpm, high-energy)	Extensive amorphisation (strong loss of crystallinity)	Reactive alumina (Al_2O_3)
(Taşkın et al., 2009)	Diaspore	Energy-Responsive Si-Al Contributors	Non-silicate (Hydroxide, α-AlO(OH))	H-bonded layers	6.5–7	Perfect	60–75 min	Planetary ball milling (600 rpm, high-energy, tungsten carbide, dry milling)	Nearly 95% amorphisation	Reactive alumina (Al_2O_3)
(Yang et al., 2005)	Illite	Energy-Responsive Si-Al Contributors	Layered Silicates	Weak K^+ interlayer bonds	1–2	Perfect	120 min	Planetary ball milling (600 rpm, high-energy, dry milling)	Extensive amorphisation (strong loss of crystallinity)	Reactive silica (SiO_2) and alumine (Al_2O_3)
(Yao et al., 2019)	Muscovite	Energy-Responsive Si-Al Contributors	Layered Silicates	Strong K^+ interlayer bonds	2.5	Perfect	160 min	Planetary ball milling (500 rpm, high-energy, dry milling)	Extensive amorphisation (relative crystallinity ↓ to 14.99%, strong dehydroxylation)	Reactive silica (SiO_2) and alumina (Al_2O_3); formation of amorphous C–S–H gel incorporating Al^{3+} and K^+
(Murouchi et al., 2021)	Wollastonite	Energy-Intensive Si-Al Contributors	Single-chain silicate	Single chains cross-linked by Ca^{2+}	4.5–5	Perfect	2 h and 317 h	Conventional ball milling (100 rpm, low-energy, dry, alumina vessel, zirconia balls)	Partial amorphization at 2 h, Extensive amorphisation at 317 h	Reactive amorphous silica (SiO_2) and Ca release
(Murouchi et al., 2021)	Diopside	Energy-Intensive Si-Al Contributors	Single-chain silicate	Single chains cross-linked by Ca^{2+}/Mg^{2+}	5.5–6	Good	2 h and 512 h	Conventional ball milling (100 rpm, low-energy, dry, alumina vessel, zirconia balls)	Partial amorphization at 2 h, Extensive amorphisation at 512 h	Reactive amorphous silica (SiO_2) and Mg release
(Alyosif et al., 2023)	Albite	Energy-Intensive Si-Al Contributors	Framework Silicate	3D Si–O–Al framework	6–6.5	Perfect	90 min	Planetary ball milling (400 rpm, high-energy, tungsten carbide, dry milling)	Extensive amorphisation (strong loss of crystallinity)	Reactive amorphous silica (SiO_2), alumina (Al_2O_3), and Na release
(Alyosif et al., 2023)	Microcline	Energy-Intensive Si-Al Contributors	Framework silicate	3D Si–O–Al framework with limited channel voids due to Al-substitution	6–6.5	Perfect	120 min	Planetary ball milling (400 rpm, high-energy, tungsten carbide, dry milling)	Extensive amorphisation (strong loss of crystallinity)	Reactive amorphous silica (SiO_2), alumina (Al_2O_3), and K release
(Wei et al., 2009)	Plagioclase	Energy-Intensive Si-Al Contributors	Framework silicate	3D Si–O–Al framework with limited channel voids	6–6.5	Perfect	8 h	Planetary ball milling (300 rpm, moderate-	Extensive amorphisation (strong loss of crystallinity)	Reactive amorphous silica (SiO_2), alumina (Al_2O_3), and Ca release

(*continued on next page*)

Table 1 (*continued*)

Ref	Mineral	Proposed Classification	Amorphization Potential Factors		Energy Requirement Factors		Milling Duration	Milling Conditions	Degree of Structural Distruption	Contribution to Cement Systems
			Bond Topology	**Structural Connectivity**	**Mohs Hardness**	**Cleavage Quality**				
				due to Al-substitution				energy, dry milling, agate media)		
(Kweon et al., 2025)	Quartz	Energy-Intensive Si-Al Contributors	Framework silicate	3D Si–O–Si framework	7	No	180 min	Planetary ball milling (200–800 rpm, ZrO_2 jar and balls, BPR 40:1, dry)	Partial amorphisation	Limited surface-derived reactive silica
(Gobindlal et al., 2021)	Quartz	Energy-Intensive Si-Al Contributors	Framework silicate	3D Si–O–Si framework	7	No	600 min	Planetary ball milling (Retsch PM100, 500 rpm, ZrO_2 jar and balls, dry)	Gradual amorphisation with extended milling	Limited surface-derived reactive silica
(Baláž et al., 2008)	Fayalite	Energy-Intensive Si-Al Contributors	Nesosilicate	Isolated SiO_4 tetrahedra linked by Fe^{2+}	6.5–7	No	30 min	Planetary ball milling (450 rpm, high-energy, tungsten carbide jar and balls, dry milling)	Nearly 83% amorphisation	Reactive silica (SiO_2) and Fe release
(Baláž et al., 2008)	Fayalite	Energy-Intensive Si-Al Contributors	Nesosilicate	Isolated SiO_4 tetrahedra linked by Fe^{2+}	6.5–7	No	120 min	Attritor milling (1500 rpm, high-energy, stainless-steel balls, wet milling)	Nearly 88% amorphisation	Reactive silica (SiO_2) and Fe release
(Baláž et al., 2008)	Fayalite	Energy-Intensive Si-Al Contributors	Nesosilicate	Isolated SiO_4 tetrahedra linked by Fe^{2+}	6.5–7	No	10 min	Nutating milling (900 rpm, moderate-energy, stainless steel balls, dry and wet milling)	Nearly 43% amorphisation (dry mode); when water was added, surface area increased sharply and amorphisation accelerated	Reactive silica (SiO_2) and Fe release
(Nadirov and Mussapyrova, 2020)	Fayalite	Energy-Intensive Si-Al Contributors	Nesosilicate	Isolated SiO_4 tetrahedra linked by Fe^{2+}	6.5–7	No	45 min	Planetary ball milling (400 rpm, high-energy, steel jar and balls, dry milling)	Partial amorphisation; crystallinity strongly decreased	Reactive silica (SiO_2) and Fe release

Note: Cleavage terminology follows standard mineralogical nomenclature used to describe preferential crystallographic fracture behaviour. Structural disruption descriptors reflect the terminology reported in the original mechanochemical studies.

Table 2
Summary of representative studies on minerals classified as "Oxide Contributors" within the proposed mechanical activation framework, including crystallographic characteristics, milling conditions, degree of amorphisation, and contribution to cementitious systems. Abbreviations: rpm, revolutions per minute.

Ref	Mineral	Proposed Classification	Amorphization Potential Factors		Energy Requirement Factors		Milling Duration	Milling Conditions	Degree of Structural Disruption	Contribution to Cement Systems
			Bond Topology	**Structural Connectivity**	**Mohs Hardness**	**Cleavage Quality**				
(Kristóf and Juhász, 1993)	Dolomite	Oxide Contributors – Carbonates-Reactivity via Calcination	Non-silicate (Carbonate)	CO_3^{2-} groups with Ca^{2+}/Mg^{2+} linkages (alternating, anisotropic)	3.5–4	Perfect	2 h	Planetary ball milling (AGO I, 1820 rpm pot / 890 rpm axle, high-intensity, steel balls, water-cooled)	Significant amorphization; lattice distortion (006 planes) but no bond rupture / no phase formation	No new product formed; only minor structural changes
(Kristóf and Juhász, 1993)	Magnesite	Oxide Contributors – Carbonates-Reactivity via Calcination	Non-silicate (Carbonate)	CO_3^{2-} groups with Mg^{2+} linkages (uniform, compact)	3.5–4.5	Perfect	2 h	Planetary ball milling (AGO I, 1820 rpm pot / 890 rpm axle, high-intensity, steel balls, water-cooled)	No major amorphisation; minor lattice strain, no phase formation	No new product formed; only minor structural changes
(Zuo et al., 2024)	Siderite	Oxide Contributors – Carbonates-Reactivity via Calcination	Non-silicate (Carbonate)	CO_3^{2-} groups with Fe^{2+} linkages (uniform, compact)	3.5–4.5	Perfect	120 min	Planetary ball milling (500 rpm, high-energy, zirconia jar, dry milling)	Very limited amorphisation; crystal structure largely retained; only minor lattice distortion	No new product formed; only minor structural changes
(Pesenti et al., 2008)	Calcite	Oxide Contributors – Carbonates-Reactivity via Calcination	Non-silicate (Carbonate)	CO_3^{2-} groups with Ca^{2++++} linkages (uniform, stable)	3	Perfect	100 h	Planetary ball milling (200 rpm, dry, 25 steel balls, 20 min milling + 60 min pause)	Partial transformation to aragonite (~40%); crystallite size reduced to < 50 nm; lattice defects introduced; no complete amorphisation	No reactive phases formed; calcite/ aragonite retained ($CaCO_3$)
(Pesenti et al., 2008)	Calcite	Oxide Contributors – Carbonates-Reactivity via Calcination	Non-silicate (Carbonate)	CO_3^{2-} groups with Ca^{2+} linkages (uniform, stable)	3	Perfect	150 min	Vibrating cup milling (1100 rpm, dry, −20 °C, 3 min milling + 5 min pause)	Peak broadening with nanoscale domain size; microstrain increased; calcite structure largely retained; no aragonite detected	No reactive phases formed; only calcite retained ($CaCO_3$)
(Bańkowska-Sobczak et al., 2024)	Calcite	Oxide Contributors – Carbonates-Reactivity via Calcination	Non-silicate (Carbonate)	CO_3^{2-} groups with Ca^{2+} linkages (uniform, stable)	3	Perfect	30 min	Planetary ball milling (Pulverisette, 250–550 rpm, dry, ball:sample = 5:1)	Slight loss of crystallinity (~4% decrease), no aragonite formed	No new product formed; calcite retained ($CaCO_3$)
(Wei et al., 2009)	Ilmenite	Oxide Contributors – Low-Reactive Oxides	Non-silicate (Oxide)	Close-packed O^{2-} lattice with Fe/Ti cations	5–6	No	4 h	Planetary ball milling (300 rpm, moderate-energy, dry milling, agate media)	Partial amorphisation (crystallite size ↓ by 50%, lattice strain ↑ by 50%)	Reactive Fe and Ti release
(Ebadi and Pourghahramani, 2019)	Ilmenite	Oxide Contributors – Low-Reactive Oxides	Non-silicate (Oxide)	Close-packed O^{2-} lattice with Fe/Ti cations	5–6	No	150 min	Planetary ball milling (450 rpm, high-energy, stainless steel, dry vs wet milling)	Nearly 95% amorphisation (dry milling, 150 min); nearly 68.6% amorphization (wet milling, 150 min)	Reactive Ti release (TiO_{222} dissolution), Fe ion release
(Basturkcu et al., 2017)	Goethite	Oxide Contributors – Low-Reactive Oxides	Non-silicate (Oxide)	Close-packed O^{2-} layers with Fe^{3+}–OH linkages	5–5.5	No	2 h	Eccentric vibratory ball milling (960 rpm, high-intensity, steel balls, dry milling)	Dehydroxylation; partial loss of crystallinity; transformation of goethite to hematite	Reactive Fe release
(Pourghahramani et al., 2008)	Hematite	Oxide Contributors – Low-Reactive Oxides	Non-silicate (Oxide, Fe_2O_3, trigonal)	Close-packed O^{2-} lattice with Fe^{3+} cations	5.5–6.5	No	9 h	Vibratory ball milling (1000 rpm, 8 mm amplitude, dry milling, air atmosphere)	81.73% amorphisation	Reactive Fe release
(Pourghahramani et al., 2008)	Hematite	Oxide Contributors – Low-Reactive Oxides	Non-silicate (Oxide, Fe_2O_3, trigonal)	Close-packed O^{2-} lattice with Fe^{3+} cations	5.5–6.5	No	9 h	Tumbling ball milling (60 rpm, dry milling, air atmosphere)	80.3% amorphisation	Reactive Fe release
(Pourghahramani et al., 2008)	Hematite	Oxide Contributors – Low-Reactive Oxides	Non-silicate (Oxide, Fe_2O_3, trigonal)	Close-packed O^{2-} lattice with Fe^{3+} cations	5.5–6.5	No	9 h	Planetary ball milling (axle 100 rpm, drum 200 rpm, dry milling, air atmosphere)	85.47% amorphisation	Reactive Fe release

Note: Cleavage terminology follows standard mineralogical nomenclature used to describe preferential crystallographic fracture behaviour. Structural disruption descriptors reflect the terminology reported in the original mechanochemical studies.

resulted in the release of CO_2 and the formation of reactive MgO and Fe-oxides (Hou et al., 2021; Pan et al., 2000). Collectively, these findings confirm that carbonate minerals contribute to cementitious reactivity only after calcination, which converts defect-enriched precursors into highly reactive oxide phases.

In the low-reactive oxides group, dense iron- and titanium-bearing oxides such as ilmenite, goethite, and hematite exhibit high resistance due to their close-packed O^{2-} lattices, but mechanical activation can still induce partial disorder and enhance dissolution, leading to the release of reactive Fe_2O_3, Fe_3O_4, and TiO_2 phases. Ilmenite (Mohs 5–6) has been reported to undergo substantial amorphisation (90–95%) within 90–150 min of planetary milling at 450 rpm, accompanied by enhanced Ti and Fe release, while lower disorder (~69%) was observed under wet milling (Wei et al., 2009; Ebadi and Pourghahramani, 2019). Goethite (Mohs 5–5.5) shows only partial crystallinity loss under vibratory milling, but progressive dehydroxylation triggers incipient hematite formation, indicating that OH groups act as weak points under stress (Falagán et al., 2017). Hematite (Mohs 5.5–6.5, trigonal Fe_2O_3 with a close-packed Fe–O framework) has been reported to amorphise gradually under dry milling, with the extent depending on the mill type: after 9 h, amorphisation reached ~ 85.47% in a planetary mill (axle 100 rpm, drum 200 rpm), ~80.3% in a tumbling mill (60 rpm), and ~ 81.73% in a vibratory mill (1000 rpm, 8 mm amplitude) (Wang et al., 2022).

Carbonate minerals confirm the necessity of calcination, since milling alone induces only defects or minor polymorphic changes without generating reactive oxides. In contrast, ilmenite and, to a lesser extent, goethite and hematite demonstrate that dense oxides can undergo defect-induced amorphisation, promoting the release of reactive Fe and Ti species. Collectively, these findings support their framework classification as Oxide Contributors with contributions to cementitious systems governed by oxide generation via thermal or mechanical activation pathways.

5.2.3. *Unsuitable Minerals*

The final category, designated as "Unsuitable Minerals", encompasses minerals whose response to mechanical activation either produces deleterious by-products or remains negligible due to exceptional

Table 3
Summary of representative studies on minerals classified as "Unsuitable Minerals" within the proposed mechanical activation framework, including crystallographic characteristics, milling conditions, degree of amorphisation and contribution to cementitious systems. Abbreviations: rpm, revolutions per minute.

Ref	Mineral	Proposed Classification	Amorphization Potential Factors		Energy Requirement Factors		Milling Duration	Milling Conditions	Degree of Structural Disruption	Contribution to Cement Systems
			Bond Topology	**Structural Connectivity**	**Mohs Hardness**	**Cleavage Quality**				
(Hu et al., 2002)	Galena	Unsuitable Minerals-Sulfide Bearing Minerals	Non-silicates (Sulfides)	Cubic ionic lattice	2.5	Perfect	260 min	Planetary ball milling (200 rpm, powder: ball = 1:25, stainless steel jar and balls, inert atmosphere)	Partial amorphisation; crystallite size decreases, lattice distortions increase	Oxidation product $PbSO_4$ formed
(Aram et al., 2021)	Sphalerite	Unsuitable Minerals-Sulfide Bearing Minerals	Non-silicate (Sulfide, ZnS)	Cubic ionic/ covalent lattice	3.5–4	Perfect	180 min	Planetary ball milling (450 rpm, high-energy, stainless-steel balls, ball: powder 15:1; wet and dry modes)	Extensive amorphisation (up to ~ 90.3% dry; ~75% wet at 180 min)	Zn^{2+} and Fe^{2+} release and sulfur vacancies formed (H_2S release)
(Pourghahramani and Akhgar, 2015)	Pyrite	Unsuitable Minerals-Sulfide Bearing Minerals	Non-silicate (Sulfide, FeS_2, cubic)	Cubic Fe–S_2 lattice	6–6.5	No	100 min	Planetary ball mill (400 rpm, stainless steel balls, Ar atmosphere, ball: powder 20:1)	~70% amorphisation	Defect-rich amorphous pyrite (no new phase formed)
(Zheng et al., 2020)	Pyrite	Unsuitable Minerals-Sulfide Bearing Minerals	Non-silicate (Sulfide, FeS_2, cubic)	Cubic Fe–S_2 lattice	6–6.5	No	120 min	Planetary ball mill (400 rpm, 15 stainless steel balls Ø20 mm)	Partial amorphisation	Fe^{3+} dissolution, sulfate formation
(Tang et al., 2025)	Pyrite	Unsuitable Minerals-Sulfide Bearing Minerals	Non-silicate (Sulfide, FeS_2, cubic)	Cubic Fe–S_2 lattice	6–6.5	No	24 h	Planetary ball mill (YXQM-1 L, MITR, 300 rpm, agate jar, ball: powder 20:1)	Crystallite size reduced, lattice strain increased, peak broadening,	Sulfur vacancies and Fe^{2+} enrichment formed
(Sen et al., 1999)	Anatase	Unsuitable Minerals-Structurally Resistant Minerals	Non-silicate (Oxide)	Close-packed O^{2-} lattice with Ti^{4+} cations	5–6	Perfect	100 h	Vibrational ball milling (SPEX 8000, 1000 rpm, dry, Al_2O_3 jar and ball)	No amorphisation; phase transformations to metastable TiO_2 (II) and TiO_2 (B)	Formation of metastable TiO_2 (II) and TiO_2 (B), with minor rutile

Note: Cleavage terminology follows standard mineralogical nomenclature used to describe preferential crystallographic fracture behaviour. Structural disruption descriptors reflect the terminology reported in the original mechanochemical studies.

Table 4
Summary of literature studies investigating the cementitious performance of mechanically activated mine tailings and their evaluation using the proposed mineral-based mechanical activation framework. Abbreviations: SSA, specific surface area; XRD, X-ray diffraction; C–S–H, calcium silicate hydrate; AFt, ettringite; rpm, revolutions per minute.

TAILINGS PROPERTIES							CEMENTITIOUS MATRIX PERFORMANCE OF TREATED TAILINGS				MINERAL-BASED ASSESSMENT	
Ref	**Tailings Type**	**Taxonomy Group**	**Chemical Composition (%)**	**Physical Properties**	**Structural State**	**Minerals**	**Optimum Replacement Level**	**Optimum Activation Duration and Milling Conditions**	**Effects of Activation**	**Results**	**Mineral-based Mechanical Activation Group of Minerals**	**Assessment of Activation Effectiveness**
(Wang et al., 2022)	Lead-zinc	Limited Latent Pozzolanic Tailings	SiO_2: 27.35 Al_2O_3: 3.32 Fe_2O_3: 6.43 CaO: 22.78 SO_3: 1.35	Particle size: 59.71 μm	Crystalline	Dolomite Muscovite Quartz Riebeckite Calcite	30% with cement	2 h dry grinding in planetary ball mill, 300 rpm	SSA ↑ (%331) D50 ↓ (%91.4) Diffraction peak intensities of crystalline phases ↓ (significantly)	Compressive Strength ↑ Strength Activity Index ↑ The binding energies of Al–O and Si–O bonds ↓ Porosity ↓	Carbonates-Reactivity via Calcination Energy-Responsive Si-Al Minerals Energy-Intensive Si-Al Minerals Energy-Intensive Si-Al Minerals Carbonates-Reactivity via Calcination	**HIGHLY SUITABLE**
(Yao et al., 2019)	Gold	Latent Pozzolanic Tailings	SiO_2: 72.86 Al_2O_3: 13.68 Fe_2O_3: 1.11 CaO: 1.06 SO_3: 0.16	SSA: 233.2 m^2/kg	Crystalline	Muscovite Microcline Albite Quartz	30% with cement	80 min dry grinding in planetary ball mill	SSA ↑ (threefold) Relative crystallinity after 80 min grinding: Muscovite: 37% **(↓ %63)** Microcline: 48.7% **(↓ %51.3)** Albite: 61.1% **(↓ %38.9)** Quartz: 80.9% **(↓ %19.1)**	Compressive Strength ↑ C-S-H Content ↑Ca$(OH)_2$ Consumption ↑ Ettringite Formation ↑ Pozzolanic Activity Index ↑ (%25.9) Porosity ↓	Energy-Responsive Si-Al Minerals Energy-Intensive Si-Al Minerals Energy-Intensive Si-Al Minerals Energy-Intensive Si-Al Minerals	**HIGHLY SUITABLE**
(Yao et al., 2020)	Iron	Latent Pozzolanic Tailings	SiO_2: 62.04 Al_2O_3: 5.8 Fe_2O_3: 22.06 CaO: 4.27 SO_3: 0.91	SSA: 103 m^2/kg	Crystalline	Quartz Muscovite Amphibole Stilpnomelane	30% with cement	40 min dry grinding, milling conditions not reported	SSA ↑ (464.1%) Amorphization levels after mechanical activation: Stilpnomelane ≅ 51% Muscovite ≅ 65%	Compressive Strength ↑ C-S-H Content ↑ (6.8-fold)Ca$(OH)_2$ Content ↓ (%69.6) Ettringite Formation ↑ Microstructure Compactness ↑ Pozzolanic Activity Index ↑ (%72.7)	Energy-Intensive Si-Al Minerals Energy-Responsive Si-Al Minerals Energy-Intensive Si-Al Minerals Energy-Responsive Si-Al Minerals	**HIGHLY SUITABLE**
(Tian et al., 2024)	Vanadium-Titanium Iron	Partly Pozzolanic Tailings	SiO_2: 43.55 Al_2O_3: 10.99 Fe_2O_3: 12.04 CaO: 15.95 SO_3: NA	D50: 70.73 μm	Partly-amophous	Mica Hornblende	30% with cement	50 min dry grinding, milling conditions not reported	SSA ↑ (2.7-fold) D50 ↓ (%82) Reactive Si^{4+} + Al^{3++} content ↑ (2.9-fold)	Compressive Strength ↑ Activity Index ↑ (%32.6) Porosity ↓ Amount of AFt ↑	Energy-Responsive Si-Al Minerals Energy-Intensive Si-Al Minerals	**HIGHLY SUITABLE**

(*continued on next page*)

Table 4 (*continued*)

TAILINGS PROPERTIES							CEMENTITIOUS MATRIX PERFORMANCE OF TREATED TAILINGS				MINERAL-BASED ASSESSMENT	
Ref	**Tailings Type**	**Taxonomy Group**	**Chemical Composition (%)**	**Physical Properties**	**Structural State**	**Minerals**	**Optimum Replacement Level**	**Optimum Activation Duration and Milling Conditions**	**Effects of Activation**	**Results**	**Mineral-based Mechanical Activation Group of Minerals**	**Assessment of Activation Effectiveness**
						Chlorite				C–S–H formation ↑	Energy-Responsive Si-Al Minerals	
						Plagioclase					Energy-Intensive Si-Al Minerals	
						Quartz					Energy-Intensive Si-Al Minerals	
						Diopside					Energy-Responsive Si-Al Minerals	
						Epidote					Structurally Resistant Minerals	
						Ilmenite					Low-Reactive Oxides	
(Wang et al., 2025)	Molybdenum	Latent Pozzolanic Tailings	SiO_2: 59.66 Al_2O_3: 9.02 Fe_2O_3: 12.89 CaO: 5.04 SO_3: 1.84	D50 ≅ 0.25–0.3 mm	Crystalline	Quartz	15% Molybdenum Tailings Powder with cement and 40% Molybdenum Tailings Sand with sand	45 min dry grinding, milling conditions not reported	SSA ↑ (≅ %940) D50 ↓ (≅ %90)	Compressive Strength ↑ Flexural Strength ↓ Porosity ↑ Shrinkage ↓ C-S-H Content ↑Ca $(OH)_2$ Consumption ↑	Energy-Intensive Si-Al Minerals	**HIGHLY SUITABLE**
						Biotite					Energy-Responsive Si-Al Minerals	
						Microcline					Energy-Intensive Si-Al Minerals	
						Hematite					Low-Reactive Oxides	
						Chlorite					Energy-Responsive Si-Al Minerals	
(Shi et al., 2024)	Iron	Partly-Pozzolanic Tailings	SiO_2: 32.76 Al_2O_3: 6.90 Fe_2O_3: 16.92 CaO: 21.70 SO_3: 9.50	D50 < 300 μm	Partly-amorphous	Quartz	20% iron tailings powder and 50% iron tailings sand with cement	2.5 h dry grinding, milling conditions not reported	SSA ↑ (511 m^2/kg) D50 ↓ (≅ 15 μm)	Compressive Strength ↑ Flexural Toughness ↑ Pore Diameter ↓ C-S-H Content ↑Ca $(OH)_2$ Consumption ↑ Chloride Permeability ↑ (Very Low)	Energy-Intensive Si-Al Minerals	**HIGHLY SUITABLE**
						Albite					Energy-Intensive Si-Al Minerals	
						Calcite					Carbonates-Reactivity via Calcination	
						Muscovite					Energy-Responsive Si-Al Minerals	
						Microcline (small amount) Magnetite (small amount)					Energy-Intensive Si-Al Minerals Low-reactive Oxides	

(*continued on next page*)

Table 4 (*continued*)

TAILINGS PROPERTIES							CEMENTITIOUS MATRIX PERFORMANCE OF TREATED TAILINGS				MINERAL-BASED ASSESSMENT	
Ref	**Tailings Type**	**Taxonomy Group**	**Chemical Composition (%)**	**Physical Properties**	**Structural State**	**Minerals**	**Optimum Replacement Level**	**Optimum Activation Duration and Milling Conditions**	**Effects of Activation**	**Results**	**Mineral-based Mechanical Activation Group of Minerals**	**Assessment of Activation Effectiveness**
(Wang et al., 2023)	Copper Slag	Partly Pozzolanic Tailings	SiO_2: 31.69 Al_2O_3: 5.51 Fe_2O_3: 49.03 CaO: 4.92 SO_3: 0.98	D50: 37,3 μm	Partly-amorphous	Fayalite Magnetite Corrundum	Up to 20% with cement	40 min, wet grinding, milling conditions not reported	SSA ↑ D50 ↓ (%95.2) Fayalite Content ↓	Compressive Strength ↑ C-S-H Content ↑Ca $(OH)_2$ Consumption ↑ Porosity ↓ Pore Diameter ↓ Microstructure Density ↑	Energy-Intensive Si-Al Minerals Low-Reactive Oxides Structurally Resistant Minerals	**HIGHLY SUITABLE**
(Wang et al., 2023)	Copper Slag	Partly Pozzolanic Tailings	SiO_2: 31.70 Al_2O_3: 5.50 Fe_2O_3: 49 CaO: 4.90 SO_3: 1	D50: 15.71 μm	Partly-amorphous	Magnetite Fayalite	20% with silica fume	1 h, wet grinding, milling conditions not reported	SSA ↑ D50 ↓ (%75) Fayalite Content ↓ (%20.6)	Compressive Strength ↑ Flexural Strength ↑ C-S-H Content ↑ CH Consumption ↑ Microstructure Density ↑ Pore Refinement ↑	Low-Reactive Oxides Energy-Intensive Si-Al Minerals	**HIGHLY SUITABLE**
(Mahajan and Muhammad, 2024)	Copper Slag	Partly Pozzolanic Tailings	SiO_2: 24.12 Al_2O_3: 5.29 Fe_2O_3: 63.13 CaO: 3.40 SO_3: 0.07	Particle size > 90 μm	Partly-amorphous (approx. 60%)	Magnetite Fayalite Quartz	10–15% with cement	510 min, dry grinding, milling conditions not reported	SSA ↑ (%40) D50 ↓ (%63) Fayalite Content ↓ (%3.4) The difference in the amorphous content was found to be minimal.	Compressive Strength ↑ C-S-H Content ↑Ca $(OH)_2$ Consumption ↑ Porosity ↓	Low-Reactive Oxides Energy-Intensive Si-Al Minerals Energy-Intensive Si-Al Minerals	**SUITABLE**
(Cheng et al., 2016)	Iron	Latent Pozzolanic Tailings	SiO_2: 75.23 Al_2O_3: 2.64 Fe_2O_3: 11.31 CaO: 1.47 SO_3: 0.08	SSA: 138 m^2/kg D50: 124.727 μm	Crystalline	Quartz Hematite Albite Edenite	40% with cement	3,5 h dry grinding in SYM-Cement test bal mill, 48 rpm	SSA ↑ (1371%) D50 ↓ (%92.45) Crystallinity of SiO_2 ↓	Compressive Strength ↑Ca $(OH)_2$ Consumption ↑ C-S-H Content ↑ Pozzolanic Activity Index ↑ Porosity ↓	Energy-Intensive Si-Al Minerals Low-Reactive Oxides Energy-Intensive Si-Al Minerals Energy-Intensive Si-Al Minerals	**SUITABLE**
(Wang et al., 2023)	Iron	Latent Pozzolanic Tailings	SiO_2: 62.26 Al_2O_3: 4.78 Fe_2O_3: 14.37 CaO: 7.76 SO_3: 0.48	SSA: 235 m^2/kg D50: 149.6 μm	Crystalline	Quartz Cordierite	10% with cement	2 h wet grinding in planetary mill, 400 rpm	D50 (median particle size) ↓ (98.5%) SSA ↑ (591.5%) The total crystallinity ↓ (62.33%) Amorphous	Compressive Strength ↑ C-S-H Content ↑Ca $(OH)_2$ Consumption ↑ Porosity ↓	Energy-Intensive Si-Al Minerals Energy-Intensive Si-Al Minerals	**SUITABLE**

(*continued on next page*)

Table 4 (*continued*)

TAILINGS PROPERTIES							CEMENTITIOUS MATRIX PERFORMANCE OF TREATED TAILINGS				MINERAL-BASED ASSESSMENT	
Ref	**Tailings Type**	**Taxonomy Group**	**Chemical Composition (%)**	**Physical Properties**	**Structural State**	**Minerals**	**Optimum Replacement Level**	**Optimum Activation Duration and Milling Conditions**	**Effects of Activation**	**Results**	**Mineral-based Mechanical Activation Group of Minerals**	**Assessment of Activation Effectiveness**
						Calcite			degree ↑ (37.67%) The binding energy of Si ↓ (0.22%), Al ↓ (0.13%), and Ca ↓ (0.06%)		Carbonates-Reactivity via Calcination	
(Cheng et al., 2024)	Iron	Latent Pozzolanic Tailings	SiO_2: 78.69 Al_2O_3: 2 Fe_2O_3: 6 CaO: 2.87 SO_3: NA	NA	Crystalline	Quartz Hematite Albite	30% with cement	3 h dry grinding, planetary mill, 360 rpm	SSA ↑ (1979.0 m^2/kg) D50 ↓ (7.49 μm)	Compressive Strength ↓ Elastic Modulus ↓ C-S-H Content ↑ Porosity ↓	Energy-Intensive Si-Al Minerals Low-Reactive Oxides Energy-Intensive Si-Al Minerals	**SUITABLE**
(Li et al., 2022)	Iron	Partly Pozzolanic Tailings	SiO_2: 24.28 Al_2O_3: 5.81 Fe_2O_3: 23.74 CaO: 12.69 SO_3: 1.58	D50: 47.63 μm	Partly-amorphous	Quartz Calcite Hematite Magnetite	40% with cement	2 h wet grinding in planetary ball mill with zirconia balls, 280 rpm	SSA ↑ D50 ↓ (%97.7)	Compressive Strength ↑ C-S-H Content ↑Ca $(OH)_2$ Consumption ↑ Porosity ↓	Energy-Intensive Si-Al Minerals Carbonates-Reactivity via Calcination Low-Reactive Oxides Low-Reactive Oxides	**SUITABLE**
(Hernández-Ramos et al., 2024)	Gold and Silver	Latent Pozzolanic	SiO_2: 67.20 Al_2O_3: 3.99 Fe_2O_3: 2.27 CaO: 24.70 SO_3: 0.12	D50: 15,55 μm	Crystalline	Quartz Calcite	15% with cement	140 min dry milling in planetary ball mill with steel balls, 400 rpm	Crystallinity ↓ (max reduction,19%) Quartz peak intensity ↓ D50 ↓ (15.55 μm → 0.91 μm)	Compressive Strength ↑ C-S-H Content ↑ Strength Activity Index: 79–87%	Energy-Intensive Si-Al Minerals Carbonates-Reactivity via Calcination	**SUITABLE**
(Gu et al., 2022)	Iron	Latent Pozzolanic Tailings	SiO_2: 75.24 Al_2O_3: 3.66 Fe_2O_3: 6.38 CaO: 4.05 SO_3: 0.05	SSA: 41.68 m^2/kg	Crystalline	Quartz Cordierite	10% with cement	3.5 h in planetary mill, 390 rpm	SSA ↑ (%5219) D50 ↓ (%96.6) XRD: Diffraction peaks ↓, peak broadening ↑	Compressive Strength ↑ C-S-H Content ↑Ca $(OH)_2$ Consumption ↑ Pozzolanic Activity Index: %74.5 Microstructure compactness ↑	Energy-Intensive Si-Al Minerals Energy-Intensive Si-Al Minerals	**SUITABLE**
(Agrawal and Gupta, 2022)	Zinc	Limited Latent Pozzolanic Tailings	SiO_2: 40.4 Al_2O_3: 3.99 Fe_2O_3: 4.61 CaO: 16.9 SO_3: NA	SSA: 230 m^2/kg	Crystalline	Dolomite Quartz	5% with cement	80–90 min, milling conditions not reported	SSA ↑ (%19.6) D50 ↓	Compressive Strength ↓ Flexural Strength ↓ Abrasion Resistance ↑	Carbonates-Reactivity via Calcination Energy-Intensive Si-Al Minerals	**UNSUITABLE**

(*continued on next page*)

Table 4 (*continued*)

TAILINGS PROPERTIES							CEMENTITIOUS MATRIX PERFORMANCE OF TREATED TAILINGS				MINERAL-BASED ASSESSMENT	
Ref	**Tailings Type**	**Taxonomy Group**	**Chemical Composition (%)**	**Physical Properties**	**Structural State**	**Minerals**	**Optimum Replacement Level**	**Optimum Activation Duration and Milling Conditions**	**Effects of Activation**	**Results**	**Mineral-based Mechanical Activation Group of Minerals**	**Assessment of Activation Effectiveness**
						Corundum				Drying Shrinkage ↓ Dynamic Elastic Modulus ↓ Energy Absorption Capacity ↓	Structurally Resistant Minerals	
(Gu et al., 2023)	Iron	Latent Pozzolanic Tailings	SiO_2: 62.25 Al_2O_3: 4.78 Fe_2O_3: 14.37 CaO: 7.76 SO_3: 0.47	SSA: 187 m^2/kg D50: 144 μm	Crystalline	Quartz	10–20% with cement	2.5 h dry grinding, planetary ball mill with steel balls, 60 rpm	SSA ↑ (%780) D50 ↓ (%88.9) No pozzolanic activity	Compressive Strength ↑ Porosity ↓ Particle Packing ↑	Energy-Intensive Si-Al Minerals	**UNSUITABLE**
(de Castro et al., 2021)	Iron	Latent Pozzolanic Tailings	SiO_2: 27.41 Al_2O_3: 3.35 Fe_2O_3: 63.27 CaO: 4.12 SO_3: NA	SSA: 5.83 m^2/g D50: 22 μm	Crystalline	Goethite (39.2%) Hematite (36.1%) Quartz (21.7%) Gibbsite (2%) Kaolinite (<1%) Magnetite (<1%)	30–40% with cement	SONNEX I-4205 ball mill, low energy milling, 14,000 turns	SSA ↑ (%33.62) D50 ↓ (%41) No significant pozzolanic activity	Compressive Strength ↑ Flexural Tensile Strength ↑ Water Absorption ↓ Porosity ↓ Carbonation Depth ↑ C-S-H Content ↑ (very low)	Low-Reactive Oxides Low-Reactive Oxides Energy-Intensive Si-Al Minerals Energy-Responsive Si-Al Minerals Energy-Responsive Si-Al Minerals Low-Reactive Oxides	**UNSUITABLE**
(Liu et al., 2022)	Iron	Partly Pozzolanic Tailings	SiO_2: 35.34 Al_2O_3: 8.47 Fe_2O_3: 17.65 CaO: 25.14 SO_3: 1.65	D50: 273.6 μm	Partly-amorphous	Quartz Calcite Andradite	30% with cement	1 h dry grinding, 300 rpm	SSA ↑ (%583.33) D50 ↓ (%95.25)	Long Term Compressive Strength ↑ C-S-H Content ↑ (very low)Ca $(OH)_2$ Content ↓ (very low) Porosity ↓ Drying Shrinkage ↓	Energy-Intensive Si-Al Minerals Carbonates-Reactivity via Calcination Structurally Resistant Minerals	**UNSUITABLE**

structural resilience. Two subgroups can be distinguished: "Sulfide-Bearing Minerals", which undergo structural degradation under milling but release sulphur species and heavy metals that compromise both durability and environmental safety; and "Structurally Resistant Minerals", which are characterised by highly stable crystallographic frameworks. Representative studies for both are summarised in Table 3.

In sulfide-bearing minerals subgroup, sulfide minerals such as galena, sphalerite, and pyrite have been consistently reported to undergo structural degradation under milling; however, their transformation products, sulfates, sulfur volatiles, and heavy-metal ions (Pb^{2+}, $Zn2^{+}$, $Fe2^{+}/Fe3^{+}$), render them incompatible with cementitious systems (Juhász and Opoczky, 1990; Pourghahramani and Akhgar, 2015; Hu et al., 2002; Zheng et al., 2020). For example, galena (PbS, Mohs 2.5) has shown progressive but incomplete amorphisation under extended milling, accompanied by defect accumulation and the release of elemental sulfur and $PbSO_4$ (Hu et al., 2002). sphalerite (ZnS, Mohs 3.5–4) has demonstrated unusually rapid amorphisation, with amorphous fractions approaching 90% under dry milling, yet this response has been linked to sulfur volatilisation and Zn leaching (Aram et al., 2021). pyrite (FeS_2; Mohs 6–6.5) has been reported to show greater resistance to mechanical activation due to its tightly bonded cubic Fe–S_2 framework. Planetary milling at 400 rpm achieved ~ 70% amorphisation after 100 min (Pourghahramani and Akhgar, 2015), while other studies reported only partial disordering after 20–120 min, with broadened diffraction peaks, sulphur vacancy formation, and defect-rich surfaces but no complete amorphisation (Zheng et al., 2020; Pourghahramani and Akhgar, 2015). Even prolonged milling up to 24 h induced only partial collapse with crystallite size reduction and lattice strain (Tang et al., 2025). Overall, sulfide-bearing minerals respond to milling primarily through defect generation and sulphur vacancy formation, processes that invariably lead to the release of heavy metals and sulphur species, thereby confirming their environmental unsuitability for cementitious use.

On the other hand, structurally resistant minerals subgroup comprises minerals with highly stable crystallographic frameworks, including anatase, corundum, epidote, and andradite. These phases, although chemically benign, possess high hardness, poor cleavage, and densely interconnected networks that resist amorphisation. Anatase (TiO_2; Mohs 5.5–6) exemplifies this subgroup, showing crystallite size reduction from ~ 120 nm to 13 nm after 100 h of vibrational milling without amorphisation (Sen et al., 1999). Instead, it undergoes polymorphic transformation to metastable TiO_2 (II) and TiO_2 (B) with minor rutile formation, a response attributed to its stable Ti–O bonding, which accommodates strain through structural reorganisation rather than lattice breakdown. Similar behaviour has been reported for corundum, epidote and andradite, which remain largely crystalline and inaccessible under practical milling conditions (Baláž, 2008; Juhász and Opoczky, 1990).

In summary, the unsuitable minerals classification captures two mechanistically distinct limitations: sulfide-bearing minerals, which are mechanically activated but yield environmentally hazardous by-products, and structurally resistant minerals, which remain inert even under intensive milling. Together, these subgroups reinforce the framework's rationale that either chemical incompatibility or structural intractability precludes effective utilisation of such minerals in cementitious systems through mechanical activation.

5.3. Empirical verification of a mineral-based mechanical activation framework for mine tailings using literature-derived data

Unlike single-mineral systems, mine tailings are multiphase mineral assemblages whose responses to mechanical processing are often nonlinear. In such heterogeneous systems, interactions among coexisting mineral phases may influence the activation behaviour and can lead to synergistic or antagonistic effects depending on mineralogical composition and relative phase abundance. Yet their activation behaviour is largely governed by the dominant mineral phases, making knowledge of individual mineral responses essential for anticipating heterogeneous performance. On this basis, a mineral-based mechanical activation framework was developed to classify minerals according to both their reactivity potential and their capacity to contribute to cementitious performance once activated. This section evaluates literature studies from the compiled database in which mechanically activated mine tailings were incorporated into cementitious matrices, to assess the framework's validity.

Building on the mineral-level analysis presented in the previous sections, the framework was further evaluated using quantitative cementitious performance indicators reported in experimental studies where mechanically activated mine tailings were incorporated into cementitious matrices. Table 4 summarises empirical investigations in which mine tailings underwent mechanical activation prior to cementitious use. In each case, the tailings' mineralogical composition was interpreted through the framework and the applied activation judged as "highly suitable", "suitable", or "unsuitable". The assessment is partly inferential, since most studies lack quantitative phase-abundance data; where necessary, dominant phases were deduced from reported cementitious performance indicators, including strength development, pozzolanic activity indices, $Ca(OH)_2$ consumption, and the type of hydration products formed (e.g., C–S–H, C–A–S–H). Secondary milling parameters such as grinding duration, atmosphere, and energy input were also considered, as they strongly influence activation efficiency.

Despite these limitations, the comparative analysis shows broad consistency between framework-based interpretations and reported experimental outcomes. The observed alignment suggests that the framework provides a useful mineralogically informed basis for interpreting the reactivity of heterogeneous tailings and guiding the selection of mechanical activation strategies.

5.3.1. Mineralogical variability and processability constraints governing the mechanical activation of heterogeneous mine tailings

This section summarizes literature in which mine tailings with varying mineralogical compositions are mechanically activated and incorporated into cementitious matrices, to evaluate the applicability of the proposed mineral-based mechanical activation framework in interpreting the activation potential.

Based on the proposed framework, studies in which the activation of mine tailings is assessed as highly suitable typically involve tailings rich in energy-responsive Si-Al minerals such as muscovite, biotite, chlorite, and stilpnomelane. These phases undergo substantial structural degradation under milling, releasing reactive silica and enhancing pozzolanic performance. For example, lead–zinc tailings (Wang et al., 2022), containing calcite, dolomite, quartz, riebeckite, and muscovite, showed partial amorphisation after 2 h of milling and corresponding pozzolanic activity gains were reported. Similarly, gold mine tailings (Yao et al., 2019), containing muscovite, albite, microcline, and quartz exhibited large reductions in crystallinity (e.g., muscovite 63%, microcline 51%, albite 38.9%) after 80 min were noted, accompanied by a 25.9% increase in pozzolanic index. Likewise, iron tailings (Yao et al., 2020), dominated by muscovite and stilpnomelane, amorphization levels of 65% and 51%, were reported accompanied by a 6.8-fold increase in C–S–H formation and a 69.6% decrease in $Ca(OH)_2$ after 40 min of milling. On the other hand, vanadium–titanium iron tailings (Tian et al., 2024), containing mica and chlorite, a 2.9-fold increase in reactive Si and a 32.6% higher activity index were reported, largely attributed to the reactivity of these phyllosilicates. In summary, these results consistently demonstrate that phyllosilicate-rich tailings are the most energy-responsive and provide reliable pozzolanic improvements under milling, confirming the robustness of the framework.

A notable exception has been observed in fayalite-rich tailings, particularly copper slag, where processability has been reported to depend strongly on milling conditions. Dry grinding has generally been found to be ineffective due to localized heating and agglomeration,

whereas wet grinding has been shown to prevent agglomeration, create defect-rich surfaces, and promote dissolution of Fe–O and Si–O bonds, thereby releasing reactive Fe^{2+} and silicate species. For instance, in copper slag (Wang et al., 2023) containing fayalite, quartz, and magnetite, only 40 min of wet grinding has been reported to markedly reduce fayalite peak intensities. This effect, attributed to surface dissolution and depolymerization rather than mechanical disruption alone, has been shown to enhance amorphization and pozzolanic reactivity, as confirmed by higher $Ca(OH)_2$ consumption and C–S–H formation. Similarly, in another study (Wang et al., 2023) on fayalite–magnetite slag, a 20.6% reduction in fayalite has been observed after 1 h of wet grinding, with released silica contributing to hydration reactions. In contrast, prolonged dry grinding (510 min) of fayalite–magnetite–quartz slag (Mahajan and Muhammad, 2024) has been reported to yield only a 3.4% reduction in fayalite and negligible amorphization, with limited pozzolanic gain. This contrast underscores the decisive role of milling parameters in determining activation outcomes. Overall, these results confirm that fayalite is highly suitable under wet grinding, fully consistent with its classification.

Studies deemed suitable for mechanical activation have typically involved tailings dominated by energy-intensive Si–Al minerals such as quartz, albite, and microcline. Due to their stable lattices, these phases have been shown to exhibit limited amorphization and only moderate pozzolanic gains unless subjected to intense milling. For example, in iron tailings with quartz, albite, edenite, and hematite, increased C–S–H and $Ca(OH)_2$ consumption has been reported after 3.5 h of dry grinding (Cheng et al., 2016), while in another study on quartz–albite–hematite tailings, improvements in C–S–H have been observed after 3 h at 360 rpm, though effectiveness remained limited (Cheng et al., 2024). In iron tailings with quartz, calcite, hematite, and magnetite, strength and hydration improvements have been reported after 2 h of high-intensity wet grinding (Li et al., 2022), reflecting the surface reactivity of quartz but only moderate overall enhancement. In gold–silver tailings (quartz and calcite), 140 min of high-energy dry grinding has been shown to reduce crystallinity by ~ 19% and raise the strength index to 79–87%, yet crystalline persistence constrained activation (Hernández-Ramos et al., 2024). Likewise, in quartz–cordierite tailings, 3.5 h of dry grinding at 390 rpm has been reported to yield strength and hydration gains, but inert corundum further limited reactivity (Gu et al., 2022). Collectively, these findings demonstrate that quartz- and feldspar-rich tailings respond effectively only under very high-energy conditions, yet the reactivity gains remain modest relative to phyllosilicate-rich systems.

According to the framework, studies classified as “not suitable” for mechanical activation typically contain tailings dominated by mineral phases from the ‘oxide contributor’ or ‘unsuitable’ groups, such as dolomite, hematite, magnetite, goethite, corundum, and andradite. Since these minerals respond poorly to mechanical activation, applying this treatment to tailings where they are dominant has generally been found to be ineffective and of limited benefit. For example, in zinc tailings (Agrawal and Gupta, 2022) containing dolomite, quartz, and corundum, 80–90 min of milling was reported to result in poor cementitious performance, with reductions in strength attributed to inert corundum and insufficient energy to activate quartz. Likewise, in iron tailings (Gu et al., 2023) dominated by quartz, 2.5 h of dry grinding at 60 rpm in a planetary mill did not produce pozzolanic activity; although improvements in compressive strength and particle packing were noted, the applied energy was inadequate to induce quartz reactivity. In another case, iron tailings (de Castro et al., 2021) rich in goethite (39.2%), hematite (36.1%), and quartz (21.7%) showed negligible pozzolanic activity and minimal C–S–H formation after low-energy milling, as the dominance of low-reactivity oxides outweighed the limited contribution of gibbsite and kaolinite. In short, tailings dominated by corundum and other low-reactivity oxides consistently fail to respond to mechanical activation, thereby verifying the framework’s classification of these phases as low-reactivity.

Overall, although chemical composition serves as the primary criterion for assessing the cementitious performance of mine tailings, their response to activation and the choice of the most effective treatment are ultimately governed by mineralogical composition. This study has demonstrated broad consistency between the proposed mineral-based framework and experimentally reported activation behaviour in heterogeneous tailings systems. Through this approach, the framework redefines activation potential as a design parameter rather than a know-how approach, providing a mechanistically informed decision-support tool for reducing reliance on energy-intensive trial-and-error activation routes and enabling resource-efficient valorisation pathways.

6. General discussion

This study introduces the first mineral-based framework for evaluating the mechanical activation of mine tailings, reframing activation not as an empirically driven approach but as a more knowledge-based and systematic design approach. The framework classifies minerals according to their potential contribution to cementitious matrices and their response to mechanical activation, grounding this classification in crystallographic and physical attributes that govern susceptibility to amorphisation. This mineral-level perspective represents a step-change in the field: it transforms mechanical activation from a generic treatment into a targeted engineering tool, thereby addressing the fundamental source of inconsistency across prior studies. Beyond cementitious applications, the framework’s mineralogical grounding renders it transferable to other mineral-based residues, offering a widely applicable approach for valorisation.

The applicability of the framework has been supported through two complementary levels of literature-based evaluation. First, literature data on individual minerals confirmed that structural attributes and bonding topology reliably dictate mechanochemical response. Phyllosilicates and hydroxides, for example, showed rapid amorphisation and strong pozzolanic activity, while quartz and feldspars required substantially higher energy input, and sulfide-bearing minerals produced deleterious by-products. Second, case studies on heterogeneous mine tailings revealed that performance outcomes could be anticipated by reference to the dominant mineral phases. Tailings rich in phyllosilicates consistently delivered significant pozzolanic improvements under milling, whereas quartz- or oxide-dominated systems yielded only modest gains. Even condition-dependent cases such as fayalite-rich slags aligned with the framework, confirming that mineralogical composition primarily governs activation response and that the framework provides a mechanistically informed basis for interpreting the behaviour of heterogeneous mine tailings, thereby guiding decision-making in both academic research and industrial practice. Nevertheless, in heterogeneous tailings systems, interactions among coexisting mineral phases may introduce synergistic or antagonistic effects that influence the activation behaviour, adding an additional layer of complexity when interpreting activation responses in real tailings assemblages.

From an industrial perspective, the implications are significant. Targeted activation strategies within the framework reduce reliance on unsystematic approaches, support energy budgeting, and avoid processing routes that are either inefficient or environmentally hazardous. In practice, this can save substantial energy costs, improve reproducibility, and accelerate the deployment of low-carbon binders. Moreover, by aligning existing specifications such as ASTM C618 (ASTM International., 2023); ASTM C1866 (ASTM International., 2020); BS EN 450–1 (British Standards Institution, 2012); CFR (40 CFR § 261.24, n. d.) and WM3 (Agency et al., 2021) thresholds, the framework establishes a structured pathway for potential integration into future standards on the utilisation of mine tailings. This facilitates cross-industry collaboration between the mining and construction industries, creating pathways for resource efficiency, reduced carbon emissions, and the advancement of circular economy principles. In this sense, the framework can support broader net-zero and circular-economy transition strategies.

At the same time, the analysis highlights critical areas for future development. Milling parameters such as mill type, rotational speed, duration, and atmosphere exert decisive influences on mechanochemical outcomes, often equal in magnitude to mineralogical factors. The lack of standardisation in reporting and optimising these parameters remains a barrier to comparability and scalability. Similarly, the development of transferable quantitative activation criteria and decision-guiding thresholds remains challenging under the current state of the literature, where mechanochemical datasets are often generated under substantially different mineralogical and processing conditions. More systematic and mineralogically resolved datasets generated under comparable experimental frameworks will therefore be essential for advancing toward more quantitative and mechanistically interpretable activation design strategies. Beyond this, bridging the gap between laboratory studies and practical deployment requires pilot-scale validation and assessment of technology readiness levels (TRLs), ensuring scalability and industrial feasibility.

This work establishes a mineral-level framework for the valorisation of mine tailings by mechanical activation. By moving beyond compositional averages and empirical trials, it provides a mechanistic basis for interpreting activation behaviour and guiding the selection of suitable processing routes. Its applicability has been evaluated through mineral-level analysis and heterogeneous tailings case studies, demonstrating its relevance for both scientific understanding and industrial application.

7. Conclusion

Chemical composition serves as the primary criterion for assessing the cementitious performance of mine tailings, but the activation response and choice of treatment are ultimately governed by mineralogical composition. This study introduced and evaluated the first mineral-based mechanical activation framework, demonstrating that crystallographic attributes such as bond topology, structural connectivity, hardness, and cleavage can be systematically translated into reactivity outcomes. Both single-mineral studies and heterogeneous tailings case analyses confirmed the decision-making competency of the framework, establishing that phyllosilicate-rich residues consistently exhibit enhanced pozzolanic reactivity, while quartz-, feldspar-, and oxide-dominated systems respond only under high-energy conditions, and sulfide-bearing phases are unsuitable.

Framework verification was undertaken using a rigorously curated subset of the literature-derived database developed in this study, comprising 19 investigations that report mechanical activation of mine tailings with sufficient mineral-specific detail to enable mineral-specific interpretation. The framework enables a knowledge-based, design-oriented strategy for mechanical activation offering a paradigm change in the valorisation of mine tailings. Its mineralogical basis provides a transferable conceptual framework for evaluating other mineral-derived residues and a scientific foundation for developing comparable mineralogically informed evaluation tools across diverse waste streams. Importantly, the framework not only advances academic understanding but also aligns with practical needs: when embedded into future standardisation pathways (e.g., ASTM C618 (ASTM International., 2023), BS EN 450–1 (British Standards Institution, 2012), it can contribute to the development of more comparable classification approaches for mine tailings in relation to conventional SCM systems and can support industry decision-making toward more resource-efficient valorisation strategies.

Equally, the framework provides a foundation upon which future pilot-scale validation and technology readiness level (TRL) advancement can be built, supporting scalability and energy-efficient deployment. The integration of mineralogical insights with empirical verification also provides a basis for future cross-industry collaboration, circular economy integration, and potential contributions toward net-zero targets. More broadly, the framework highlights how mineralogical insights can support the development of more structured and systematic waste valorisation pathways.

Funding Statement

This work was supported by the Royal Society of Edinburgh (RSE) Research Collaboration Grant (Ref: RSE 6037). Additional financial support was provided by the Heriot-Watt University Small Project Grants Scheme.

CRediT authorship contribution statement

Berika Ceren Cihan Yılmaz: Writing – original draft, Validation, Methodology, Investigation, Formal analysis, Data curation, Conceptualization. **Demetrios M. Cotsovos:** Supervision, Conceptualization. **Gavin Mudd:** Visualization, Conceptualization. **Richard J. Ball:** Writing – original draft, Visualization, Formal analysis, Conceptualization. **Ceren Ince:** Writing – original draft, Visualization, Supervision, Methodology, Formal analysis, Conceptualization.

Declaration of competing interest

The authors declare that they have no known competing financial interests or personal relationships that could have appeared to influence the work reported in this paper.

Acknowledgement

We sincerely thank Rachel Paul, Business Unit Leader for Mineral Resource Management at Acrux Gold, for her valuable insights and for providing key information that supported the development of this review. This work was supported by the Royal Society of Edinburgh (RSE) through a Research Collaboration Grant (Ref: RSE 6037), and by the Heriot-Watt University Small Project Grants Scheme (October 2025).

Data availability

No data was used for the research described in the article.

References

OECD. (2018). Global material resources outlook to 2060: Economic drivers and environmental consequences — Highlights.
Vidal, O., Goffé, B., Arndt, N., 2013. Metals for a low-carbon society. Nat. Geosci. 6 (11), 894–896. https://doi.org/10.1038/ngeo1993.
Jasansky, S., Lieber, M., Giljum, S., Maus, V., 2023. An open database on global coal and metal mine production. Sci. Data 10 (1), 1–12. https://doi.org/10.1038/s41597-023-01965-y.
Nguyen, R.T., Eggert, R.G., Severson, M.H., Anderson, C.G., 2021. Global electrification of vehicles and intertwined material supply chains of cobalt, copper and nickel. Resour. Conserv. Recycl. 167, 105198. https://doi.org/10.1016/j.resconrec.2020.105198.
Anglo American. (n.d.). What are minerals used for? https://www.angloamerican.com/futuresmart/stories/our-industry/our-products/uses-of-minerals.
Reichl, C., Schatz, M., 2025. World mining data 2025. In: Federal Ministry of Finance, Vol. 40.
World Gold Council. (n.d.). The authority on gold. https://www.gold.org/.
OECD. (2024). Global critical minerals outlook 2024. https://www.oecd.org/critical-minerals/.
Copper demand set to soar 70% by 2050: Can supply keep up? (n.d.). https://www.miningvisuals.com/post/copper-demand-in-2050.
Humphreys, D., 2020. Mining productivity and the fourth industrial revolution. Miner. Econ. 33 (1–2), 115–125. https://doi.org/10.1007/s13563-019-00172-9.
Global Tailings Portal. (n.d.). Global tailings portal. https://tailing.grida.no/.
Concas, A., Ardau, C., Cristini, A., Zuddas, P., Cao, G., 2006. Mobility of heavy metals from tailings to stream waters in a mining activity contaminated site. Chemosphere 63 (2), 244–253. https://doi.org/10.1016/j.chemosphere.2005.08.024.
Budianta, W., 2021. Heavy metal pollution and mobility of sediment in Tajum River caused by artisanal gold mining in Banyumas, Central Java. Indonesia. Environmental Science and Pollution Research 28 (7), 8585–8593. https://doi.org/10.1007/s11356-020-11157-5.
Li, W., Deng, Y., Wang, H., Hu, Y., Cheng, H., 2024. Potential risk, leaching behavior and mechanism of heavy metals from mine tailings under acid rain. Chemosphere 350, 140995. https://doi.org/10.1016/j.chemosphere.2023.140995.

Lottermoser, B.G., 2011. Recycling, reuse and rehabilitation of mine wastes. Elements 7 (6), 405–410. https://doi.org/10.2113/gselements.7.6.405.
Serbula, S.M., Milosavljevic, J.S., Radojevic, A.A., Kalinovic, J.V., Kalinovic, T.S., 2017. Extreme air pollution with contaminants originating from the mining–metallurgical processes. Sci. Total Environ. 586, 1066–1075. https://doi.org/10.1016/j.scitotenv.2017.02.091.
Afif, C., Chélala, C., Borbon, A., Abboud, M., Adjizian-Gérard, J., Farah, W., Jambert, C., Zaarour, R., Saliba, N.B., Perros, P.E., Rizk, T., 2008. SO in Beirut: Air quality implication and effects of local emissions and long-range transport. Air Quality, Atmosphere & Health 1 (3), 167–178. https://doi.org/10.1007/s11869-008-0022-y.
Piciullo, L., Storrøsten, E.B., Liu, Z., Nadim, F., Lacasse, S., 2022. A new look at the statistics of tailings dam failures. Eng. Geol. 303, 106657. https://doi.org/10.1016/j.enggeo.2022.106657.
Islam, K., Murakami, S., 2021. Global-scale impact analysis of mine tailings dam failures: 1915–2020. Glob. Environ. Chang. 70, 102361. https://doi.org/10.1016/j.gloenvcha.2021.102361.
Chronology of major tailings dam failures. (n.d.). https://www.wise-uranium.org/mdaf.html.
CBS News. (n.d.). Cement industry accounts for about 8% of CO_2 emissions. One startup seeks to change that. https://www.cbsnews.com/news/cement-industry-co2-emissions-climate-change-brimstone/.
Kinnunen, P., Karhu, M., Yli-Rantala, E., Kivikytö-Reponen, P., Mäkinen, J., 2022. A review of circular economy strategies for mine tailings. Cleaner Eng. Technol. 8, 100499. https://doi.org/10.1016/j.clet.2022.100499.
Scrivener, K., Martirena, F., Bishnoi, S., Maity, S., 2018. Calcined clay limestone cements (LC3). Cem. Concr. Res. 114, 49–56. https://doi.org/10.1016/j.cemconres.2017.08.017.
Lottermoser, B. G. (2010). Mine wastes: Characterization, treatment and environmental impacts (3rd ed.).
González-Díaz, E., García, S., Soto, F., Navarro, F., Townley, B., Caraballo, M.A., 2022. Geochemical, mineralogical and geostatistical modelling of an IOCG tailings deposit (El Buitre, Chile): Implications for environmental safety and economic potential. J. Geochem. Explor. 239, 106997. https://doi.org/10.1016/j.gexplo.2022.106997.
Falagán, C., Grail, B.M., Johnson, D.B., 2017. New approaches for extracting and recovering metals from mine tailings. Miner. Eng. 106, 71–78. https://doi.org/10.1016/j.mineng.2016.10.008.
Fashola, M.O., Ngole-Jeme, V.M., Babalola, O.O., 2016. Heavy metal pollution from gold mines: Environmental effects and bacterial strategies for resistance. Int. J. Environ. Res. Public Health 13 (11), 1047. https://doi.org/10.3390/ijerph13111047.
Hu, L., Wu, H., Zhang, L., Zhang, P., Wen, Q., 2017. Geotechnical properties of mine tailings. J. Mater. Civ. Eng. 29 (2), 04016220. https://doi.org/10.1061/(ASCE)MT.1943-5533.0001736.
Nascimento, S.C., Parbhakar-Fox, A., Cracknell, M.J., Cooke, D.R., Miller, C.B., Heng, W. X., 2023. Geochemical, mineralogical, and geophysical methods to establish the geoenvironmental characteristics of the King River delta, Queenstown. Western Tasmania. Applied Geochemistry 159, 105820. https://doi.org/10.1016/j.apgeochem.2023.105820.
Saberi, N., Vriens, B., 2025. Compositional heterogeneity of secondary minerals in mine waste rock: Origins and implications for water quality. J. Hazard. Mater. 487, 137163. https://doi.org/10.1016/j.jhazmat.2025.137163.
Lindsay, M.B.J., Moncur, M.C., Bain, J.G., Jambor, J.L., Ptacek, C.J., Blowes, D.W., 2015. Geochemical and mineralogical aspects of sulfide mine tailings. Appl. Geochem. 57, 157–177. https://doi.org/10.1016/j.apgeochem.2015.01.009.
Nascimento, S.C., Cooke, D.R., Cracknell, M.J., Miller, C.B., Parbhakar-Fox, A., 2025. Mineralogical and geochemical characterization of mine tailings in the King River delta, Western Tasmania: Implications for long-term stability of trace elements. Appl. Geochem. 184, 106366. https://doi.org/10.1016/j.apgeochem.2025.106366.
40 CFR § 261.24. (n.d.). Toxicity characteristic. https://www.ecfr.gov/current/title-40/chapter-I/subchapter-I/part-261/subpart-C/section-261.24.
Environment Agency, Scottish Environment Protection Agency, & Natural Resources Wales. (2021). Waste classification: Guidance on the classification and assessment of waste (Technical Guidance WM3, 1st edition v1.2 GB). https://www.gov.uk/government/publications/waste-classification-technical-guidance-wm3.
ASTM International. (2023). ASTM C618: Specification for coal fly ash and raw or calcined natural pozzolan for use in concrete. doi: 10.1520/C0618-23.
ASTM International. (2020). ASTM C1866/C1866M-20: Standard specification for ground-glass pozzolan for use in concrete. doi: 10.1520/C1866_C1866M-20.
British Standards Institution. (2012). BS EN 450-1:2012 Fly ash for concrete — Definitions, specifications and conformity criteria.
Wang, Y., Hu, Y., Yang, J., He, Y., He, X., Su, Y., Strnadel, B., 2023. Performance of cement-based materials incorporating ultra-fine copper slag. Construction and Building Materials 402, 132949. https://doi.org/10.1016/j.conbuildmat.2023.132949.
Liu, B., Meng, H., Pan, G., Zhou, H., Li, D., 2022. Relationship between the fineness and specific surface area of iron tailing powder and its effect on compressive strength and drying shrinkage of cement composites. Construction and Building Materials 357, 129421. https://doi.org/10.1016/j.conbuildmat.2022.129421.
Wang, H., Ju, C., Zhou, M., Zheng, F., Dong, Y., Hou, H., Liu, S., 2022. Grinding kinetics of lead–zinc tailing powders and its optimal particle size as a pozzolanic admixture in cement mortar. Advanced Powder Technology 33 (9), 103730. https://doi.org/10.1016/j.apt.2022.103730.
Yao, G., Liu, Q., Wang, J., Wu, P., Lyu, X., 2019. Effect of mechanical grinding on pozzolanic activity and hydration properties of siliceous gold ore tailings. Journal of Cleaner Production 217, 12–21. https://doi.org/10.1016/j.jclepro.2019.01.175.
Yao, G., Wang, Q., Wang, Z., Wang, J., Lyu, X., 2020. Activation of hydration properties of iron ore tailings and their application as supplementary cementitious materials in cement. Powder Technology 360, 863–871. https://doi.org/10.1016/j.powtec.2019.11.002.
Tian, X., Wang, C., Asrah, H., Han, L.C., Zheng, Y., 2024. Investigating the grinding characteristics of vanadium–titanium iron ore tailings for sustainable utilization in cementitious material preparation. Alexandria Engineering Journal 101, 78–89. https://doi.org/10.1016/j.aej.2024.05.057.
Baláž, P., 2008. Mechanochemistry in nanoscience and minerals engineering. Springer, Berlin Heidelberg. https://doi.org/10.1007/978-3-540-74855-7.
Avvakumov, E., Senna, M., Kosova, N., 2002. Soft mechanochemical synthesis: a basis for chemical technologies. Kluwer Academic Publishers. https://doi.org/10.1007/b114163.
Boldyrev, V.V., 2006. Mechanochemistry and mechanical activation of solids. Russian Chemical Reviews 75 (3), 177–189. https://doi.org/10.1070/rc2006v075n03abeh001205.
Feng, W., Yu, Z., Bao, R., Xiong, J., Yan, K., Liu, R., Zhang, R., Lu, X., 2024. Manufacture of tailings-based cementitious materials: Insights into tailings activation strategies. Construction and Building Materials 439, 137194. https://doi.org/10.1016/j.conbuildmat.2024.137194.
Boldyrev, V.V., Tkáčová, K., 2000. Mechanochemistry of solids: past, present, and prospects. Journal of Materials Synthesis and Processing 8 (3–4), 121–132.
Juhász, A. Z., & Opoczky, L. (1990). Mechanical activation of minerals by grinding: Pulverizing and morphology of particles. Ellis Horwood Limited / Halsted Press.
Pourghahramani, P., Akhgar, B.N., 2015. Characterization of structural changes of mechanically activated natural pyrite using XRD line profile analysis. International Journal of Mineral Processing 134, 23–28. https://doi.org/10.1016/j.minpro.2014.11.005.
Pourghahramani, P., 2006. Effects of grinding variables on structural changes and energy conversion during mechanical activation using line profile analysis (LPA) (Licentiate thesis). Luleå University of Technology, Division of Mineral Processing.
Wei, L., Hu, H., Chen, Q., Tan, J., 2009. Effects of mechanical activation on the HCl leaching behavior of plagioclase, ilmenite and their mixtures. Hydrometallurgy 99 (1–2), 39–44. https://doi.org/10.1016/j.hydromet.2009.06.003.
Ebadi, H., Pourghahramani, P., 2019. Effects of mechanical activation modes on microstructural changes and reactivity of ilmenite concentrate. Hydrometallurgy 188, 38–46. https://doi.org/10.1016/j.hydromet.2019.06.001.
Alex, T.C., Kumar, R., Roy, S.K., Mehrotra, S.P., 2014. Mechanically induced reactivity of gibbsite: Part 1. Planetary Milling. Powder Technology 264, 105–113. https://doi.org/10.1016/j.powtec.2014.05.028.
Deer, W.A., Howie, R.A., Zussman, J., 2013. An introduction to the rock-forming minerals, (3rd ed.). The Mineralogical Society.
Momma, K., Izumi, F., 2011. VESTA 3 for three-dimensional visualization of crystal, volumetric and morphology data. Journal of Applied Crystallography 44 (6), 1272–1276. https://doi.org/10.1107/S0021889811038970.
Rygel, M., 2010. Mineral cleavage. Wikimedia Commons. Available at: https://commons.wikimedia.org/wiki/File:Mineral-cleavage.gif (accessed 12 March 2026).
González-Velázquez, J.L., 2018. Fractography and Failure Analysis Vol. 3. https://doi.org/10.1007/978-3-319-76651-5.
Mindat.org. (n.d.). Mindat mineral database. Retrieved August 2, 2025, from https://www.mindat.org/.
St. John, J. (2021). Quartz 12. Wikimedia Commons. Available at: https://commons.wikimedia.org/wiki/File:Quartz_12_(from_James_St._John).jpg (Accessed: 11 March 2026).
Butyagin, P.Y., 1994. Problems in mechanochemistry and prospects for its development. Russian Chemical Reviews 63 (12), 965–976. https://doi.org/10.1070/rc1994v063n12abeh000129.
OpenGeology.org. (n.d.). 13 crystal structures – Mineralogy. Retrieved October 24, 2025, from.
Andrić, L., Terzić, A., Aćimović-Pavlović, Z., Pavlović, L., Petrov, M., 2014. Comparative kinetic study of mechanical activation process of mica and talc for industrial application. Composites Part b: Engineering 59, 181–190. https://doi.org/10.1016/j.compositesb.2013.12.003.
Baki, V.A., Ke, X., Heath, A., Calabria-Holley, J., Terzi, C., Sirin, M., 2022. The impact of mechanochemical activation on the physicochemical properties and pozzolanic reactivity of kaolinite, muscovite and montmorillonite. Cement and Concrete Research 162, 106962. https://doi.org/10.1016/j.cemconres.2022.106962.
Yao, G., Zang, H., Wang, J., Wu, P., Qiu, J., Lyu, X., 2019. Effect of mechanical activation on the pozzolanic activity of muscovite. Clays and Clay Minerals 67 (3), 209–216. https://doi.org/10.1007/s42860-019-00019-y.
Murouchi, Y., Okuno, M., Sasaki, N., 2021. Amorphization of wollastonite and diopside by ball milling. Scientific Reports of Kanazawa University 65, 17–30. https://doi.org/10.24517/0002000261.
Alyosif, B., Uysal, T., Erdemoğlu, M., 2023. Potassium chloride recovery from mechanically activated microcline through the chlorination roasting and leaching route. Physicochemical Problems of Mineral Processing 59 (5), 167500. https://doi.org/10.37190/ppmp/167500.
Gobindlal, K., Zujovic, Z., Yadav, P., Sperry, J., Weber, C.C., 2021. The mechanism of surface-radical generation and amorphization of crystalline quartz sand upon mechanochemical grinding. The Journal of Physical Chemistry C 125 (38), 20877–20886. https://doi.org/10.1021/acs.jpcc.1c06069.
Kweon, J.J., Khim, H., Kim, Y.-H., Lee, S.K., 2025. Structural transition in crystalline SiO_2 during mechanical amorphization under frictional shear. Journal of Materials Chemistry A 13 (28), 22672–22684. https://doi.org/10.1039/d5ta03462k.
Baláž, P., Turianicová, E., Fabián, M., Kleiv, R.A., Briančin, J., Obut, A., 2008. Structural changes in olivine $(Mg,Fe)_2SiO_4$ mechanically activated in high-energy mills. International Journal of Mineral Processing 88 (1–2), 1–6. https://doi.org/10.1016/j.minpro.2008.04.001.

Šepelák, V., Myndyk, M., Fabián, M., Silva, K.L.D., Feldhoff, A., Menzel, D., Ghafari, M., Hahn, H., Heitjans, P., Becker, K.D., 2012. Mechanosynthesis of nanocrystalline fayalite, Fe_2SiO_4. Chemical Communications 48 (90), 11121–11124. https://doi.org/10.1039/c2cc36370d.

Nadirov, R., Mussapyrova, L., 2020. Effect of mechanical activation on leachability of fayalite in sulfuric acid solution. Current Physical Chemistry 10 (2), 82–87. https://doi.org/10.2174/1877946810666200128152729.

Alex, T.C., Kumar, R., Roy, S.K., Mehrotra, S.P., 2014. Towards ambient pressure leaching of boehmite through mechanical activation. Hydrometallurgy 144–145, 99–106. https://doi.org/10.1016/j.hydromet.2014.01.017.

Taşkın, E., Yıldız, K., Alp, A., 2009. Direct alkaline leaching of mechanically activated diasporic bauxite. Mining, Metallurgy & Exploration 26 (4), 222–225. https://doi.org/10.1007/bf03402542.

Yang, H., Yang, W., Hu, Y., Du, C., Tang, A., 2005. Effect of mechanochemical processing on illite particles. Particle & Particle Systems Characterization 22 (3), 207–211. https://doi.org/10.1002/ppsc.200500953.

Pesenti, H., Leoni, M., Scardi, P., 2008. XRD line profile analysis of calcite powders produced by high-energy milling. Zeitschrift Für Kristallographie – Supplements 27, 143–150. https://doi.org/10.1524/zksu.2008.0019.

Bańkowska-Sobczak, A., Pryputniewicz-Flis, D., Idźkowski, J., Kozłowicz, Ł., Brenk, G., Diduszko, R., Ostrowska, A., Burska, D., 2024. Mechanical activation of a natural calcite for enhanced orthophosphate sorption. Desalination and Water Treatment 320, 100583. https://doi.org/10.1016/j.dwt.2024.100583.

Ban, M., Luxbacher, T., Lützenkirchen, J., Viani, A., Bianchi, S., Hradil, K., Rohatsch, A., Castelvetro, V., 2021. Evolution of calcite surfaces upon thermal decomposition, characterized by electrokinetics, in-situ XRD, and SEM. Colloids and Surfaces a: Physicochemical and Engineering Aspects 624, 126761. https://doi.org/10.1016/j.colsurfa.2021.126761.

Jiménez, A., Rives, V., Vicente, M.A., 2022. Thermal study of the hydrocalumite–katoite–calcite system. Thermochimica Acta 713, 179242. https://doi.org/10.1016/j.tca.2022.179242.

Kristóf, É., Juhász, A.Z., 1993. The effect of intensive grinding on the crystal structure of dolomite. Powder Technology 75 (2), 145–152. https://doi.org/10.1016/0032-5910(93)80075-l.

Olszak-Humienik, M., Jabłoński, M., 2015. Thermal behavior of natural dolomite. Journal of Thermal Analysis and Calorimetry 119 (3), 2239–2248. https://doi.org/10.1007/s10973-014-4301-6.

Zuo, Q., Yang, Y., Xie, X., Yang, L., Zhang, Q., He, X., 2024. Grinding siderite with ferric sulfate to generate an active ferrous source for Cr(VI) reduction. Chemosphere 361, 142516. https://doi.org/10.1016/j.chemosphere.2024.142516.

Hou, Q., Luo, X., Li, M., An, D., Xie, Z., 2021. Non-isothermal kinetic study of high-grade magnesite thermal decomposition and morphological evolution of MgO. International Journal of Applied Ceramic Technology 18 (3), 765–772. https://doi.org/10.1111/ijac.13708.

Pan, Y., Zhu, R., Banerjee, S.K., Gill, J., Williams, Q., 2000. Rock magnetic properties related to thermal treatment of siderite: Behavior and interpretation. Journal of Geophysical Research: Solid Earth 105 (B1), 783–794. https://doi.org/10.1029/1999jb900358.

Basturkcu, H., Açarkan, N., Göck, E., 2017. The role of mechanical activation on atmospheric leaching of a lateritic nickel ore. International Journal of Mineral Processing 163, 1–8. https://doi.org/10.1016/j.minpro.2017.04.001.

Pourghahramani, P., Pålsson, B., Forssberg, E., 2008. Multivariate projection and analysis of microstructural characteristics of mechanically activated hematite in different grinding mills. International Journal of Mineral Processing 87 (3–4), 73–82. https://doi.org/10.1016/j.minpro.2008.02.002.

Hu, H., Chen, Q., Yin, Z., Zhang, P., Tang, A., 2002. Oxidation behavior of mechanically activated galena in thermogravimetry (TG). Thermochimica Acta 395 (1–2), 139–144. https://doi.org/10.1016/s0040-6031(02)00142-9.

Zheng, X., Cao, S., Nie, Z., Chen, J., Ling, W., Liu, L., Pan, X., Yang, H., Xia, J., 2020. Impact of mechanical activation on bioleaching of pyrite: a DFT study. Minerals Engineering 148, 106209. https://doi.org/10.1016/j.mineng.2020.106209.

Aram, R., Abdollahy, M., Pourghahramani, P., Darban, A.K., Mohseni, M., 2021. Dissolution of mechanically activated sphalerite in the wet and dry milling conditions. Powder Technology 386, 275–285. https://doi.org/10.1016/j.powtec.2021.03.011.

Pourghahramani, P., Akhgar, B.N., 2015. Influence of mechanical activation on the reactivity of natural pyrite in lead(II) removal from aqueous solutions. Journal of Industrial and Engineering Chemistry 25, 131–137. https://doi.org/10.1016/j.jiec.2014.10.023.

Tang, L., Leng, Z., Li, S., Zheng, L., Huang, Y., Dai, W., Lin, W., Li, L., Sun, S., 2025. Ball-milled natural pyrite activating persulfate to degrade alachlor: Mechanistic elucidation and degradation pathways. Separation and Purification Technology 378, 134479. https://doi.org/10.1016/j.seppur.2025.134479.

Sen, S., Ram, M.L., Roy, S., Sarkar, B.K., 1999. The structural transformation of anatase TiO_2 by high-energy vibrational ball milling. Journal of Materials Research 14 (3), 841–848. https://doi.org/10.1557/jmr.1999.0112.

Wang, Y., Yuan, Z., Yang, J., He, Y., He, X., Su, Y., Strnadel, B., 2023. Utilization of ultra-fine copper slag to prepare eco-friendly ultrahigh-performance concrete by replacing silica fume. Construction and Building Materials 406, 133476. https://doi.org/10.1016/j.conbuildmat.2023.133476.

Mahajan, D.S., Muhammad, S., 2024. Assessment of the viability of pozzolanic activity of copper slag for use as supplementary cementitious material in ordinary Portland cement. Journal of Building Engineering 83, 108375. https://doi.org/10.1016/j.jobe.2023.108375.

Cheng, Y., Huang, F., Li, W., Liu, R., Li, G., Wei, J., 2016. Test research on the effects of mechanochemically activated iron tailings on the compressive strength of concrete. Construction and Building Materials 118, 164–170. https://doi.org/10.1016/j.conbuildmat.2016.05.020.

Cheng, Y., Ma, H., Zhang, J., 2024. Effects of siliceous iron tailings powder on performances of the interface transition zone in concrete. Construction and Building Materials 421, 135764. https://doi.org/10.1016/j.conbuildmat.2024.135764.

Li, H., Wang, R., Wei, M., Lei, N., Sun, H., Fan, J., 2022. Mechanical properties and hydration mechanism of high-volume ultra-fine iron ore tailings cementitious materials. Construction and Building Materials 353, 129100. https://doi.org/10.1016/j.conbuildmat.2022.129100.

Hernández-Ramos, S.M., Trejo-Arroyo, D.L., Cholico-González, D.F., Rodríguez-Torres, G.M., Zárate-Medina, J., Vega-Azamar, R.E., León-Patiño, C.A., Ortíz-Lara, N., 2024. Characterization and effect of mechanical and thermal activation in mining tailings for use as supplementary cementitious material. Case Studies in Construction Materials 20, e02770. https://doi.org/10.1016/j.cscm.2023.e02770.

Gu, X., Zhang, W., Zhang, X., Li, X., Qiu, J., 2022. Hydration characteristics investigation of iron tailings blended ultra-high-performance concrete: the effects of mechanical activation and iron tailings content. Journal of Building Engineering 45, 103459. https://doi.org/10.1016/j.jobe.2021.103459.

Agrawal, Y., Gupta, T., 2022. Examining the effect of particle modification on zinc tailing waste as a cementitious material in concrete: Performance and toxicity assessment. Journal of Material Cycles and Waste Management 24 (3), 1156–1171. https://doi.org/10.1007/s10163-022-01388-8.

Gu, X., Liu, B., Li, Z., Wang, H., Liu, J., Nehdi, M.L., Zhang, Y., 2023. Mechanical grinding kinetics and particle packing–based novel characterization of iron ore tailings as inert filler for cement mortar. Journal of Building Engineering 78, 107558. https://doi.org/10.1016/j.jobe.2023.107558.

de Castro, N.L.B., Almada, B.S., Fajardo, A.A., Oliveira, C.A., dos Santos, W.J., 2021. Influence of addition contents of iron ore tailings on structural mortar. Journal of Management and Sustainability 11 (1), 74–82. https://doi.org/10.5539/jms.v11n1p74.

Wang, Y., Zhuge, Y., Yao, Y., 2025. Design and performance analysis of ultra-high-performance concrete using fully recycled molybdenum tailings waste. Construction and Building Materials 473, 140981. https://doi.org/10.1016/j.conbuildmat.2025.140981.

Shi, J., Pan, W., Kang, J., Yu, Z., Sun, G., Li, J., Zheng, K.K., Shen, J., 2024. Properties of ultra-high-performance concrete incorporating iron tailings powder and iron tailings sand. Journal of Building Engineering 83, 108442. https://doi.org/10.1016/j.jobe.2024.108442.

Wang, H., Gu, X., Liu, J., Zhu, Z., Wang, S., Xu, X., Meng, J., 2023. Enhancement mechanism of micro–iron ore tailings on mechanical properties and hydration characteristics of cement–steel slag system. Journal of Building Engineering 79, 107882. https://doi.org/10.1016/j.jobe.2023.107882.